AD-A144 853 AUTOMATED AIRCRAFT ICING FORECAST TECHNIQUE(U) AIR 1/1
FORCE GLOBAL WEATHER CENTRAL OFFUTT AFB NE M Y MANSUR
31 MAY 84 AFGWC-PR-84-001 SBI-AD-E850 732

UNCLASSIFIED F/G 4/2 NL

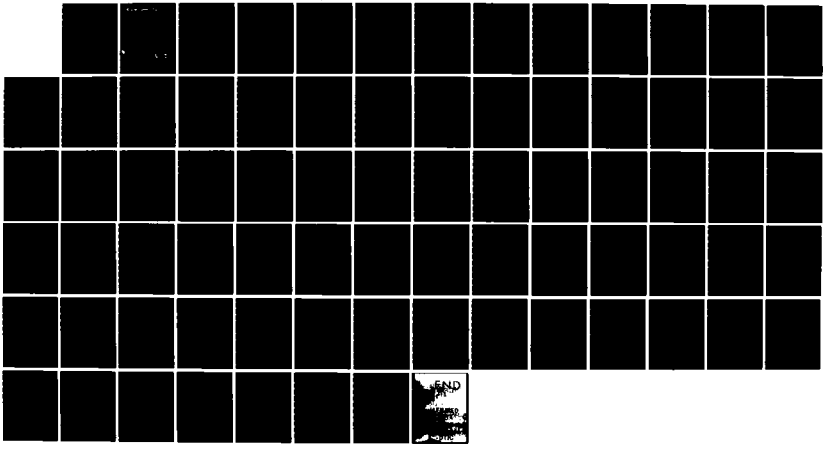

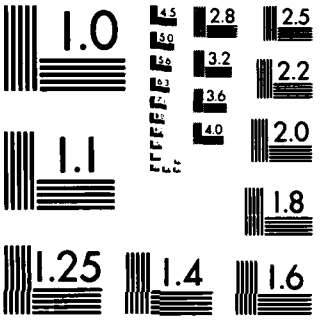

AFGWC/PR-84/001

AUTOMATED

AIRCRAFT ICING FORECAST TECHNIQUE

PROJECT REPORT

By

CAPT M. VANCE MANSUR

MAY 1984

UNITED STATES AIR FORCE
AIR WEATHER SERVICE (MAC)
AIR FORCE GLOBAL WEATHER CENTRAL
OFFUTT AFB NE 68113

REVIEW AND APPROVAL STATEMENT

This publication approved for public release. There is no objection to unlimited distribution of this document to the public at large, or by the Defense Technical Information Center (DTIC) or the National Technical Information Service (NTIS).

This technical publication has been reviewed and is approved for publication.

Charles W. Cook

CHARLES W. COOK, GM-13
Reviewing Official

FOR THE COMMANDER

Peter J. Havanac

PETER J. HAVANAC, Lt Col, USAF
Chief, Technical Services Division

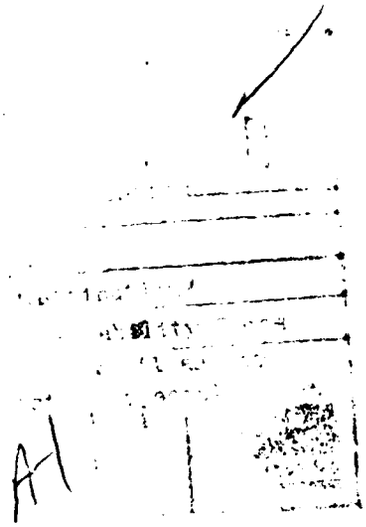

UNCLASSIFIED

SECURITY CLASSIFICATION OF THIS PAGE

AD-A144 502

REPORT DOCUMENTATION PAGE

1a. REPORT SECURITY CLASSIFICATION Unclassified	1b. RESTRICTIVE MARKINGS
2a. SECURITY CLASSIFICATION AUTHORITY	3. DISTRIBUTION/AVAILABILITY OF REPORT Approved for public release; distribution unlimited.
2b. DECLASSIFICATION/DOWNGRADING SCHEDULE	
4. PERFORMING ORGANIZATION REPORT NUMBER(S) AFGWC/PR-84/001	5. MONITORING ORGANIZATION REPORT NUMBER(S)
6a. NAME OF PERFORMING ORGANIZATION Air Force Global Weather Central 6b. OFFICE SYMBOL (If applicable) AFGWC/TS	7a. NAME OF MONITORING ORGANIZATION
6c. ADDRESS (City, State and ZIP Code) Offutt AFB, Nebraska 68113	7b. ADDRESS (City, State and ZIP Code)
8a. NAME OF FUNDING/SPONSORING ORGANIZATION 8b. OFFICE SYMBOL (If applicable)	9. PROCUREMENT INSTRUMENT IDENTIFICATION NUMBER
8c. ADDRESS (City, State and ZIP Code)	10. SOURCE OF FUNDING NOS. PROGRAM ELEMENT NO. / PROJECT NO. / TASK NO. / WORK UNIT NO.
11. TITLE (Include Security Classification) Automated Aircraft Icing Forecast Technique Project Report	
12. PERSONAL AUTHOR(S) Mansur, M. Vance	
13a. TYPE OF REPORT Final 13b. TIME COVERED FROM _____ TO _____	14. DATE OF REPORT (Yr., Mo., Day) 84-05-31 15. PAGE COUNT 73
16. SUPPLEMENTARY NOTATION This Project Report provides a comprehensive overview of the state of the art in icing.	

17 COSATI CODES		
FIELD	GROUP	SUB. GR.
04	02	

18. SUBJECT TERMS (Continue on reverse if necessary and identify by block number)
Aircraft icing, liquid water, drop size, icing forecast, dew-point depression, pseudo-isentropic lift

19. ABSTRACT (Continue on reverse if necessary and identify by block number)

This Project Report provides a comprehensive overview of the state of the art in icing forecasting and its associated problems. It describes the attempt to automate a manual icing forecast technique. The weaknesses, software design and algorithms are discussed. Attempts to filter out what was felt to be excess areal coverage, as produced by other automated procedures was unsuccessful. Moderating the filtering resulted in a sieve effect with no better results than forecasts already produced by other automated methods. Final examination revealed other reasons for the poor performance in the automated mode. The manual technique had the advantage of human pattern recognition which is vastly superior to the coarse mesh grid data used in this study, as well as access to frontal positions. There were some valuable lessons learned regarding theoretical limitations to skill scores and the inherent limitations of the models.

20. DISTRIBUTION/AVAILABILITY OF ABSTRACT UNCLASSIFIED/UNLIMITED ☒ SAME AS RPT. ☐ DTIC USERS ☐	21. ABSTRACT SECURITY CLASSIFICATION Unclassified
22a. NAME OF RESPONSIBLE INDIVIDUAL Charles W. Cook	22b. TELEPHONE NUMBER (Include Area Code) 402-294-5520 22c. OFFICE SYMBOL AFGWC/TS

DD FORM 1473, 83 APR EDITION OF 1 JAN 73 IS OBSOLETE

UNCLASSIFIED

SECURITY CLASSIFICATION OF THIS PAGE

PREFACE

This Project Report provides a comprehensive overview of the state of the art in icing forecasting and its associated problems. Additional problems arising from the automation of icing forecasts are also discussed. The analysis and forecast models at Air Force Global Weather Central which support the existing Diagnostic Weather Element (DWE) icing forecast are examined and their bias toward analyzing and forecasting too much moisture and cloud is noted. The inputs, logic, and outputs of DWE are examined followed by the introduction of a manual technique based on four case studies.

The object of this project was to automate the manual technique as described in a functional description and then test the validity of the automated version which was named Automated Icing (AUTICE). As described in the functional description AUTICE is essentially DWE with cloud, vorticity advection, vertical velocity, and pseudo-isentropic lift criteria added to filter out what was felt to be excess areal coverage by DWE. The weaknesses of AUTICE, its software design, and its algorithms were discussed.

Initially the new technique had too strong of a filter. Attempts to moderate the filtering resulted in a sieve effect which caused AUTICE to strongly resemble DWE. The filtering extremes were caused by the lack of overlap between the dew-point and cloud criteria and between the three lift criteria. Both models had equal false alarm rates but AUTICE's extreme filtering caused it to miss 94 percent of the RAOB analyzed areas. By contrast, DWE hit 44 percent of those areas and was close to 22 percent of the remaining areas.

In addition to the strong filtering, an examination of one of the manual technique case studies revealed other reasons for the poor performance in the automated mode. First the manual technique had the advantage of human pattern recognition which was vastly superior to coarse mesh grids in the two areas examined. Also the manual technique used actual clouds and winds and had access to frontal positions.

Solving the icing problem has been a personal interest from my earliest days as an Air Weather Service detachment forecaster. Many thanks are due to Lt Col Robert G. Feddes who alerted me to this opportunity to automate and test a manual technique developed by Major Harry D. White. Thanks are also due to Lt Jason P. Tuell and Major Paul F. Demmert for their advice, comments and assistance with this project. Finally, I must also thank the Computer Display Development Section of AFGWC and Lt Tuell whose Sperry and FORTRAN knowledge in "debugging" the code helped immeasurably to reduce the automation portion of my task down to a manageable size.

Captain M. Vance Mansur
31 May 1984

TABLE OF CONTENTS

LIST OF FIGURES

1. History and Scope of the Icing Forecast Problem

AWS/TR-80/001, Forecasters' Guide on Aircraft Icing, (1980) (hereafter referred to as TR-80) is the technical basis for forecasting aircraft icing in Air Weather Service (AWS) units. Data used in developing TR-80 were obtained on AWS weather reconnaissance flights over the North Atlantic, North Pacific, and Arctic Oceans from May 1952 to June 1955. These observations were taken using C-54 and C-119 aircraft at 700 mb and 500 mb. Therefore, TR-80 is designed primarily for reciprocating engine, straight-wing, transport aircraft operating at middle levels. The problems this and other considerations pose in producing an icing forecast are as follows:

1.1 Inadequate Scope The most obvious inadequacy is the limited scope of the research on which TR-80 is based. The present inventory of military aircraft operate over a greater range of levels and speeds. In some instances, individual aircraft may have larger ranges of speed and altitude for a single flight. Also, the present aircraft inventory has a greater range of aerodynamic shape.

1.2 Inadequate Observational Data Base The primary sensing device for deriving our observational data base is the rawinsonde, a balloon-carried device which measures pressure altitude, temperature, relative humidity, and by tracking the device from the ground, wind direction and speed. Use of data from the rawinsonde network to forecast icing presents two types of problems as discussed below.

1.2.1 Inadequate Density There are 71 rawinsonde stations in the upper air network in the continguous 48 states which equates to an average grid size of 332 km. To forecast any meteorological parameter, observations must be made on a grid equal to or smaller than the grid scale of the forecasts. The number and kinds of observations are not sufficient to adequately describe the icing envelope, and the forecaster must work with available data keeping in mind that he is obligated to warn pilots of any suspected icing.

1.2.2 Inadequate Parameters Rawinsondes measure the wrong parameters. In order for ice to form, the droplet (or drop) must be below freezing when it impacts the aircraft surface. Very small droplets may be carried in the airstream around the aircraft and never impact; thus one important factor is the degree to which an aerodynamic shape can collect water drops. The collection efficiency is a function of the size distribution of the water drops and the aerodynamic characteristics of the aircraft. Even though a droplet is supercooled in the cloud, compressive heating as it impacts the surface may heat it to above freezing temperatures. Such heating is a function of aircraft velocity and the aerodynamic configuration of the aircraft. The severity of icing, if it does occur, is dependent on the amount of condensed water in the supercooled state that is present in the cloud. For a complete determination of the occurence of ice it would be necessary to know:

- Collection efficiency of all parts of the aircraft as a function of aerodynamic design and speed;

- Compressive heating over all parts of the aircraft as a function of aerodynamic design and speed;

- Temperature of the cloud drops;

- Liquid water content of the cloud; and

- Size distribution of the cloud droplets.

The question arises as to how well these parameters are known. According to the National Transportation Safety Board (NTSB) (1981) pages 8-9, the Lewis Research Center and the FAA perform wind tunnel and airborne spray rig icing tests. However, this is not done for all airframes and it does not look closely enough at drop size spectra. Compressive heating is well known and available from such sources as TR-80 Figs. 8 to 11. Temperatures, as previously mentioned, are available from the rawinsonde network. Thus, the first three criteria are somewhat known but as discussed below the remaining two (liquid water content and drop size distribution) are almost totally unknown.

1.2.2.1 Liquid Water Content Throughout the Air Weather Service Skew T, Log P diagrams are analyzed for icing type and intensity using plastic overlays based on the following formula from TR-80, page 5-1, for cumuliform liquid water content:

$$LWC = (W_0 - W_1)P/(2.87T) \quad (1)$$

where
LWC = liquid water content at flight level in [g m^{-3}]
W_0 = saturation mixing ratio at cloud base [g kg^{-1}]
W_1 = saturation mixing ratio at flight level [g kg^{-1}]
P = atmospheric pressure at flight level [mb]
T = cloud temperature at flight level [°K]
2.87 = (10^2 Pa/mb)/287 [J kg^{-1} $°K^{-1}$].

This formula assumes the following: the forecaster knows the level of the cloud base, that there is an updraft with no entrainment, that no liquid falls out of the cloud, and that none of the liquid glaciates or is evaporated into the surrounding environment. In using the overlay, it is further assumed that stratiform clouds have half the liquid water content (1) calls for and that the droplet diameter for stratiform cloud will be 14 microns (cumuliform is assumed to have a 17 micron droplet size). Because it is a worst case forecast based on a coarse gridded observational network, such icing forecasts generally cover a significantly larger volume of the atmosphere than that which probably contains icing.

Besides (1) there have been several other attempts to model liquid water content. Touart (1979) evaluated two models from the Air Force Geophysics Laboratories (AFGL) and the Smith-Feddes model. All three models infer atmospheric liquid water content from conventional weather data. Their performance for 11 stations in the USSR was compared on the basis of a large sample. Touart found large differences in amounts of liquid water being forecast. However, for want of independent measurements of water content, no light was shed on the absolute accuracy of any of these models.

One flaw in all the above LWC models is their inability to handle glaciation. Temperature, dew-point, and cloud criteria perform well in

locating cold clouds; but, once located, no further tools are available to discriminate between non-glaciated cold clouds and glaciated cold clouds. Considering this, we see that state-of-the-art techniques must be limited to large area worst case forecasting.

1.2.2.2 Drop Size Distribution The same problem occurs with drop size distribution which also is neither routinely measured nor well handled by conventional models. As noted by the NTSB (1981), the few instruments currently available for measuring liquid water content and drop size distribution are primarily used for research. Generally, they all have limitations. Some will measure liquid water content but not drop size distribution. Others are limited in the range of values measured. In almost all cases, these instruments are too complex and expensive for the number of observations which would be required for synoptic use.

1.3 Compounded Error Because the parameters needed for a complete determination of the occurence of icing are unavailable, they must be inferred from those conventional parameters which are available. For the sake of illustration, assume that the needed liquid water contents and drop size distributions are 100 percent skillful in predicting icing where skill is defined as the number of correct Yes-No predictions divided by the total number of predictions. If we next assume that conventional parameters are only 80 percent skillful in inferring the liquid water contents and drop sizes (see TR-80 pages 6-2 to 6-3 and Fig 7.5 of this report) then the maximum theoretical skill in forecasting icing would be 80 percent. Finally, if we assume that conventional parameter forecasts are themselves only 80 percent skillful at 12 hours and 50 percent skillful at 48 hours, then the ultimate icing forecast suffers from compounded error. The maximum theoretical skill of an icing forecast would be 64 percent (80% x 80%) at 12 hours and 40 percent (80% x 50%) at 48 hours.

1.4 Inadequate Verification Verification is essential for developing forecast skill. It provides the feedback necessary for fine tuning a forecast model. The only two sources of icing forecast verification routinely available are PIREPs and Skew T, Log P analysis. The problems with Skew T analysis have already been discussed in paragraph 1.2.2.1. PIREPs are inadequate for forecast verification for the following reasons:

a. According to the NTSB (1981), the Subcommittee for Aviation Meteorological Services of the Federal Coordinator for Meteorological Services and Supporting Research has defined icing intensities in terms of the aircraft's ability to de-ice. Thus, reports of identical icing conditions may range from severe icing for aircraft with no de-ice capability (e.g., T-38, T-37, A-10, UH-1, and HH-53 aircraft) to light icing for aircraft well equipped to handle icing.

b. To cope with this problem, intensities are forecast in terms of the operational effect upon reciprocating engine, straight-wing transport aircraft such as the C-54 and C-118. The pilot must translate that forecast into the operational impact on his airframe. The fallacy here is that the pilot's airframe will be collecting different sized droplets than the C-54 or the C-118 on which the forecast is based. The implicit assumption is that all clouds have the same drop size spectrum!

c. Matters become further complicated by the pilot, having received a forecast for a C-54 airframe, reporting back in terms of the icing impact on his particular airframe.

d. PIREPs lack the statistical purity needed for model development. They are biased and contaminated because many pilots are unversed in the intensity definitions, because positive encounters get reported more often than negative encounters, and because research aircraft try to fly into icing conditions whereas other aircraft avoid them.

e. Finally, PIREPs are often more sparse than RAOBs, are rarely located at grid points, rarely occur on forecast verification hours, and are often unusable without subjective interpretation/qualification.

2. Automated Icing Forecast Problems at Air Force Global Weather Central

At AFGWC the process of making an icing forecast begins by collecting observational data to form a data base. Analysis models convert the observations into gridded analysis fields. In turn, forecast models use the analysis fields to produce forecast fields. The raw observations are stored in the Regions Data Base. The analysis and forecast fields are stored in the Fields Data Base. After the data bases have been built, applications models such as the currently operational Diagnostic Weather Elements (DWE) use the data to make tailored forecasts. Clearly in the case of ultimately deriving an icing forecast, all the previously mentioned problems in addition to the new problems to be discussed below create ample opportunity for more compounding of error.

2.1 High Level View of DWE Processing Figures 2.1 and 2.2 illustrate the flow of data and its processing as related to the creation of the present DWE icing forecast and the proposed Automated Icing Forecast (AUTICE). As indicated in Fig 2.1, the analysis and forecast models and the Three Dimensional Neph analysis (3DNEPH) and the Real Time Neph Analysis (RTNEPH), hereinafter referred to as 3DNEPH, send data to the Fields Data Base where it is stored in a literal named "XTGWCF." [Note, AFGWC data bases are addressed by "literal" and "label" in analogous fashion to the addressing of postal mail by state and city.] The labels (TTAZLL through TTAWLL) contain data as indicated in Fig. 2.1. The Northern Hemispheric Five Layer Model (NH5LYR) uses the cloud analysis produced by 3DNEPH and the position and pressure coordinates (x, y, p) from the forecast models to make cloud and dew-point depression forecasts which are stored in XTGWCF. DWE then accesses the temperature, cloud, dew-point depression, and gridded wind data to make its forecast. (To be strictly accurate, DWE gets its data from half mesh fields instead of the whole mesh XTGWCF.)

2.2 3DNEPH Problems 3DNEPH's sole purpose is to analyze clouds as well as possible for certain geographical areas. As a result, it is fine tuned on a daily basis. When fine tuning fails to produce the desired results in these areas, human beings manually insert cloud data. This manual insertion is referred to as "bogusing." Two problems arise when secondary customers such as DWE use 3DNEPH and NH5LYR data for their purposes. First, the 3DNEPH tropical and mid-latitude tuning factors can have a cumulative effect which causes an over-analysis of clouds. Second, the bogusing is normally limited only to the areas of interest. To use an analogy, 3DNEPH sees the world through an astigmatic lens. The lens gives the best image technically possible in the areas of interest but other areas are distorted.

2.3 NH5LYR Problems NH5LYR uses the 3DNEPH cloud analysis and the position and pressure coordinates from other models to produce cloud and dew-point depression forecasts. This is accomplished through five processes.

2.3.1 Process 1 In the first process indicated in Fig 2.2, NH5LYR uses empirically derived curves to convert the 3DNEPH cloud analysis to condensation pressure spread (CPS). CPS is the number of millibars a cloudless parcel must be lifted to reach saturation (positive CPS) or the number of millibars a cloudy parcel must subside to dissipate (negative CPS).

2.3.2 Process 2 The question arises, "How many millibars will parcels arriving at 850, 700, or 500 mb at some future time have risen/subsided in

moving from their present locations to the forecast grid points?" Process 2 answers this by using location and pressure coordinates (x, y, p) and winds to compute a trajectory which steps back in 3 hour increments. The computed pressure change (Δ p) will be negative for rising motion.

2.3.3 Process 3 This process adds the analyzed CPS at the start of the trajectory to Δp thereby computing the CPS at forecast time.

2.3.4 Process 5 The CPS technique works well when going from cloud to CPS to cloud since the variance in the data used to produce the CPS curves is already accounted. However, CPS values in NH5LYR are also used in process 5 to infer the dew-point temperature. Since CPS curves were derived by comparing cloud data to CPS, the dew-point temperature conversion suffers. The bias tends toward too much moisture.

2.3.5 Summary of NH5LYR Problems The end result is that NH5LYR forecasts too much cloud cover and dew-point depressions that are too low. When passed on to DWE, these cloud and moisture excesses cause it to forecast too much icing. Suggestions for improving the NH5LYR forecast include:

a. Develop CPS curves for dew-point temperatures by latitude and season.

b. Bogus the 3DNEPH over the entire globe instead of just the areas of interest.

c. Develop new tuning factors for the 3DNEPH to reduce the over-interpretation of clouds in the analysis.

2.4 The DWE Forecast. DWE (Fig. 2.2 and 2.3) processes AFGWC temperature, cloud, dew-point depression, and gridded winds using the TR-80 rules on pages 6-2 and 6-3 and produces the GN2CIC map on a data control terminal (DCT) at AFGWC. The model uses four decisions (Fig. 2.3) in order to arrive at the forecast icing type and intensity. It first checks the temperature, then the dew-point depression, then the cloud type, and finally the type of advection. The model does not handle the positions of fronts and pressure centers nor does it determine the conditions for freezing precipitation. As a result, it cannot predict the severe icing intensities associated with these phenomena. This does not prevent the forecaster who is aware of these phenomena from manually modifying the forecast.

It should be noted that DWE does not check cloud amount which in theory gives rise to the possibility that DWE could forecast icing in clear areas. In practice, however, the dew-points produced by NH5LYR and used by DWE are derived from NH5LYR clouds. Thus, a dew-point depression of 4° C or less will always be associated with 1 percent or more clouds.

3. Perceived Problems/Proposed Solutions

The perception held by some in AFGWC was that NH5LYR/DWE forecasted icing mainly in areas of moist, unstable air undergoing cold air advection. Thus, the model found thunderstorms in areas of large scale subsidence. AFGWC already had good thunderstorm forecasts which implicitly included icing in the thunderstorm forecast. Thus, the model failed to forecast icing in the areas it was really needed. A second perception was that DWE forecast icing over too large of an area with too light of an intensity. These perceptions were substantiated by four case studies [Whiton, 1984].

Since AFGWC is required to forecast aircraft icing not associated with convective activity, a manual technique was developed whereby 1000 to 850 mb thermal advection and 1000 mb flow were used to find areas of increasing warm air advection called "pseudo-isentropic lift" (PILIFT). It was assumed that synoptic scale nimbostratus formed in overrunning warm fronts and occlusions would be located in these areas. Once the general area of lift was determined, the forecaster used the vertical velocities (omegas) and the positive vorticity advection (PVA) to reduce the areal coverage and fine tune the intensity. In this manner, TR-80 rule 5 on page 6-3 calling for light rime 300 nm ahead of a warm front could be used.

The proposed solution to the DWE weakness was to automate the manual technique. DWE could locate the icing in the cold advection and the new model could locate the icing in the warm advection. As an added improvement, geostrophic winds would replace the gridded winds in forecasting advection patterns. It was felt that geostrophic winds would be stronger and thus better define the advection pattern. The proposed criteria for the new model were given to me in the form of a functional description. My job was to automate it and test its meteorological goodness.

4. Criteria for the Proposed Automated Icing Program (AUTICE)

AUTICE is a Northern Hemispheric, coarse mesh, Yes-No icing forecast valid over the AUTICE octagon (Appendix A) at 850, 700, and 500 mb at 6, 12, 18, 24, 36, and 48 hours beyond data base time. In order to make a "Yes" forecast at a grid point, six criteria had to be simultaneously met. A discussion of each criterion and its justification (or lack thereof) follows.

4.1 Temperature The temperature criterion calls for temperatures between 0° C and -16° C. This criterion infers the presence of supercooled droplets. At warmer temperatures, the droplets would not be supercooled. At colder temperatures, enough droplets would glaciate to make icing unlikely.

In regard to the lower limit of 0° C, two points must be kept in mind. First, as pointed out in TR-80 paragraph 11, supercooling must exceed aerodynamic heating. For most aircraft in flight, this would decrease the value from 0° C to -2° C. On the other hand, a case can be made in favor of keeping the cutoff point at 0° C or even warmer because of the low compressional heating for helicopters which are very sensitive to icing and for slow moving aircraft on final approach and takeoff which is the most dangerous part of flight. In the case of induction icing, the partial vacuum created around the compressor intake can induce icing in temperatures as warm as 5° C.

The -16° C cutoff point at the other end of the temperature scale is less easily justified. Wallace and Hobbs (1977) page 183 Figure 4.27 give a graph of median freezing temperature versus drop diameter. Drops may freeze at any temperature between 0° C and -40° C depending on droplet size, amount of solute, and amount of ice nucleating materials in the droplet. The smaller the droplet, the lower the freezing temperature will be. However, the smaller the droplet, the more likely it will be to flow around the aircraft rather than impacting on it. Thus for aircraft with obtuse edges (C-54 and C-118) -16° C might be more appropriate. TR-80 and the NTSB (1981) page 4 indicate that icing should be forecast as low as -22° C. Most icing occurs at temperatures of -16° C and warmer but, nevertheless, the NTSB tests aircraft down to -22° C. The AUTICE functional description called for -16° C in an attempt to cure the DWE problem of forecasting for too large of an area.

4.2 Dew-Point Depression The dew-point depression criterion calls for dew-point depressions of 4° C or less. This criterion infers the presence of water clouds. It has been validated both empirically and theoretically. Empirical justification comes from the Project Cloud-Trail flights referenced in AWS/TR-79/006 (1979) paragraph 7.7. These flights made pressure altitude measurements of cloud heights within 2 hours and 30 nm of rawinsonde launchings. It was found that typical dew-point depressions in clouds are 1° C to 2° C at temperatures of 0° C. Whereas for temperatures between -10° C and -20° C the dew-point depression in clouds was found to be 4° C. In another study also referenced in AWS/TR-79/006 (1979) paragraph 7.7, 1027 rawinsonde observations for January 1953 at 29 US Weather Bureau stations were analyzed. For the 850-600 mb layer a 5° C dew-point depression was found to be the 50 percent delineator for broken to overcast cloud probability and a dew-point depression of 2° C was found to be the 80 percent delineator.

Theoretical justification for a 4° C dew-point depression comes from two areas. First, rawinsondes use lithium-chloride elements or carbon elements to

measure humidity from which the dew-point is derived. According to AWS/TR-79/006 paragraph 7.5.1., all three of the lithium-chloride element errors (i.e., lag, polarization, and washout) cause the reported humidity to be too low. Second, in mixed phase clouds the dew-point will be between the temperature and the frost-point. Since the frost point approximately equals nine tenths the temperature measured in degrees Celsius, it follows that at -50° C a dew-point depression of 4° C represents a super-saturation with respect to the ice crystals in the cloud. Hence, if the temperature error were 4° C, the cumulative effect at -50° C could be a reported dew-point depression of 8° C in clouds! This theoretical possibility was in fact born out in the previously mentioned January 1953 study where 5 percent to 10 percent of the dew-point depressions measured in cloud were 6° C and more.

Instead of calling for a flat 4° C icing criterion, TR-80 paragraph 36 rule 2 calls for dew-point depressions of 2° C or less at temperatures 0° C to -7° C, 3° C or less at temperatures -8° C to -15° C, and 4° C or less at temperatures -16° C to -22° C. For temperatures colder than -22° C no icing should be forecast regardless of the dew-point depression. It is surprising that the AUTICE functional description, which in other cases attempts to compensate for the excess cloud and moisture of NH5LYR, calls for a more lenient 4° C depression independent of temperature.

Regarding dew-point depressions one vital question must go unanswered, "How do NH5LYR dew-point depressions relate to cloud cover?" From the previous discussion, we know how to forecast clouds and icing given rawinsonde dew-point depressions. Until something similar to Project Cloud-Trails is done for NH5LYR, this question will remain unanswered. In the interim my first guess is that NH5LYR will be more moist than rawinsonde reports.

4.3 Cloud Cover The cloud cover criterion calls for 4/8 or more cloud at the forecast level. This criterion may be viewed as a fail-safe redundancy to further qualify the dew-point depression's inference of clouds. I have found nothing in the literature regarding the amount of cloud cover needed to sustain a given icing intensity. The 4/8 cloud cover criterion is a common sense number rather arbitrarily chosen. If AUTICE forecasts severe icing at a level but the cloud cover is only 1/10, then the aircraft will be in the cloud only 10 percent of the time and the icing will not have much operational impact. Thus, some number greater than 1/10 must be picked for the criterion.

The big impact of the cloud cover criterion comes not from the choice of coverage but rather from the choice of how to relate it to the other criteria. For a worst case forecast, points meeting either the dew-point depression or the cloud criteria would have a "yes" forecast. Whereas, for a best case forecast, a point would have to meet both criteria. In an effort to reduce the large area forecast by DWE, AUTICE goes with the best case approach and requires not only these two but that all six criteria must be met.

4.4 Omega This criterion calls for upward vertical velocities of 1 mb hr^{-1} or more which equates to an omega of -1 mb hr^{-1} or less. This is the first of three vertical velocity criteria designed to filter out points where glaciation is likely. "Unless there is sufficient upward vertical motion to maintain continuous production of supercooled liquid-water droplets, the cloud will generally change its phase with time from a liquid-water cloud to a mixed water-and-ice cloud and finally to an ice-crystal cloud." [TR-80 paragraph 31.a]

Heymsfield (1975) empirically derived equations for two curves (Fig. 4.1) which relate upward vertical velocity U in cm/s to the temperature T in degrees Celsius in stratus clouds with cloud-top temperatures lower than -20° C. The lower curve is given by:

$$U = -5.0T - .14T^2. \quad (2)$$

For vertical velocities less than specified by (2) the cloud will be completely glaciated. The upper curve is given by:

$$U = -6.5T - .16T^2. \quad (3)$$

Vertical velocities greater than those specified by (3) virtually assure the presence of liquid water. For velocities between the two curves, liquid water may or may not be present. Thus, for temperatures below -5° C, (3) requires vertical velocities of 28.5 cm s^{-1} or more to maintain liquid water. Using the conversions derived in Appendix B, this equates to omegas of -66 mb hr^{-1} at 500 mb, -93 mb hr^{-1} at 700 mb, and -113 mb hr^{-1} at 850 mb. This may be compared with velocities reported by Riehl (1981).

By comparison a cold front with a slope of 1/50 and a vertical wind shear of 40 knots up through the frontal surface would have vertical velocities of 41 cm s^{-1} which would equate to -163 mb hr^{-1} at 850 mb. Similarly, a warm front with a slope of 1/200 and a vertical wind shear up through the frontal surface of 20 knots would have a vertical velocity of 5.15 cm s^{-1} which equates to -20 mb hr^{-1} at 850 mb. It follows then that frontal lift will be only marginally adequate in producing the vertical velocities required to maintain liquid water in clouds between -5° C and -25° C.

Hence, additional mechanisms in the form of orographic lift, convection, or rainbands [Hobbs et. al. 1980a, 1980b] must also be present to maintain icing conditions following initial cloud formation.

In view of the above considerations it is interesting that the AUTICE functional description should choose -1 mb hr^{-1} as its criterion. The primary reasoning behind this is that the models which produce the omegas are too coarse to catch frontal lift. It is rather rare in fact to see omegas below -5 mb hr^{-1}. Thus, the apparent discrepancy between (2) and (3) as opposed to the -1 mb hr^{-1} criterion is strictly one of scale. The -1 mb hr^{-1} criterion stipulates that icing should be forecast only in areas of synoptic scale lift. The assumption here is that synoptic scale vetical velocity correlates with meso-scale vertical velocity. Though this may be a good assumption in areas of conditional instability, it is probable that the two velocity scales correlate only weakly when evaluated over the entire globe. Thus, synoptic scale omegas as produced by GWC models probably provide only a weak skill in forecasting glaciation.

4.5 500 mb Positive Vorticity Advection The 500 mb PVA criterion simply requires that vorticity advection be positive. The reasoning behind this lift criterion is similar to that for the omega criterion. On a synoptic scale, it rules out points with neutral or negative vorticity advection which probably will not meet the meso-scale lift requirements. The remaining points may or may not meet the meso-scale requirements. Thus PVA has the same problems omega has in locating meso-scale vertical velocity of the required magnitude.

4.6 Pseudo-Isentropic Lift This newly coined term is given by the formula:

$$-\vec{V}\cdot\nabla(-\vec{V}\cdot\nabla T) \qquad (4)$$

where V is wind velocity and T is temperature. Since the criterion calls for this value to be positive, the units of V and T are immaterial. The physical interpretation of this parameter is that warm air advection must be occuring at the point and must be increasing with time. Hence it is the advection of the thermal advection field.

As already mentioned, pseudo-isentropic lift (PILIFT) is a newly coined parameter. There is no literature that either recommends or discourages its use. PILIFT was invented to locate the warm air advection associated with warm frontal surfaces. Consequently, at any pressure level PILIFT would occur where the pressure level intersected the warm frontal surface. This forecast area is indicated in Figure 4.2. There are at least four limitations/weaknesses in trying to use PILIFIT to locate warm frontal lift:

a. PILIFT, by definition, is restricted to areas of increasing warm air advection. Consequently, AUTICE will never forecast icing in areas of cold air advection, neutral advection, or decreasing warm air advection. This limitation was recognized in the functional description. It was interpreted as a strength since the present DWE forecast already forecasts icing for the cold advection areas.

b. An unanticipated characteristic of PILIFT is that in addition to locating warm frontal surfaces it locates the upwind sides of cold cores and the downwind sides of warm cores. This is illustrated in Figure 4.3 where the wind barb represents flow aloft. The "K" indicates a thermal cold core, and the "W" represents a warm core.

c. Another unanticipated problem is that warm advection in a lower layer will not create instability and consequent meso-scale lift if the next higher layer has equal or greater amounts of warm air advection. Unfortunately, the patterns of PILIFT for the 1000 to 850 mb layer tend to overlap with the PILIFT patterns for the 850 to 700 mb layer. Thus what really needs to be examined is differential advection by height and associated changes in lapse rate.

d. The final problem is that fronts are meso-scale and that the coarse mesh octagon fields are synoptic scale. Fronts can easily be lost between grid points spaced 381 km apart. Maps of PILIFT over the Northern Hemisphere (Figs. 4.4, 4.5) are commonly two, three, and even six gridpoints wide in a given layer. Comparison of Figs. 4.4 and 4.5 with the surface frontal positions in Fig. 4.6 show that the PILIFT parameter is finding something much larger than the intersection of a warm-frontal surface with a pressure surface.

e. Though it is not a limitation or a weakness of the PILIFT parameter, one thing must be pointed out: AFGWC forecasters already have frontal positions available for overlaying on the icing forecast map. Consequently the entire motivation for adopting PILIFT (i.e., for finding warm frontal surfaces) vanishes.

5. Problems with the AUTICE Functional Description

5.1 Right Solution to the Wrong Problem As explained in paragraph 3, the AUTICE functional description was designed to solve DWE's problem of forecasting icing only in areas of cold air advection and subsidence. The solutions were to add PILIFT in order to find warm advection and to add omegas and PVA in order to find lift. Thus DWE would be used to forecast icing in areas of cold advection and AUTICE would be used to forecast icing in the areas of warm advection which DWE missed. These are good solutions but unfortunately are solutions to the wrong problem. As indicated in the decision tree for DWE (Fig 2.3), forecasts are made in areas of warm air advection. Further, there is nothing in the DWE decision tree to rule out icing forecasts in areas of lift. The problems with PILIFT have already been discussed in paragraph 4.6.

5.2 Wrong Solution to the Right Problem DWE does have a problem with forecasting icing for too broad of an area. However, as already explained in paragraph 2.2 and 2.3, 3DNEPH produces too much cloud and NH5LYR in converting the cloud to dew-points generates too large of a dew-point. This is complicated by the bias not being uniform over the globe. Thus, it is analogous to looking through astigmatic lenses. This is a valid problem. It needs to be solved. The AUTICE solution is to start with the DWE criteria (temperature and dew-point) and then qualify it with a filter in the form of clouds and three lift mechanisms. Thus, continuing the analogy, the solution to the astigmatism problem is to prescribe sunglasses to filter out the problem. Unfortunately, the filter as described in the functional description is uniform over the globe--the distortion doesn't get corrected. The preferred solution is to bogus the entire globe and to develop a better method of fine tuning 3DNEPH. Another problem which develops is that the filter is too strong. Theoretically any one of the three forms of lift should suffice. To forecast no icing when one form of lift is missing but the others are strong constitutes excessive filtering. At the other extreme, requiring only one lift criterion to be met creates too weak of a filter and the forecast begins to resemble DWE. See paragraph 7.2 for more details.

5.3 Unwarranted Assumption AUTICE assumes that weak synoptic to global scale lift forecast by the AFGWC models will correlate with the synoptic to meso-scale lift required to continually resupply a glaciating cloud with liquid water. Since the meso-scale lifts must be an order of magnitude larger (see paragraph 4.4), this assumption may not be warranted. Theoretically, synoptic scale lift would enhance meso-scale lift and might even create meso-scale lift in areas of conditional instability. However, there is no empirical evidence to justify such an assumption. DWE, on the other hand, uses temperature advection to adjust its forecast. Whether theoretically justified or not, it is based on 900 actual cases as referenced in TR-80 page 4-3. Similar empirical evidence for the three lift mechanisms should be accumulated prior to implementing them in an operational model. This requirement for empirical validation should not be surprising in view of the fact that the cutoff points for all the currently accepted criteria (temperature, dew-point depression, and thermal advection) also had to be empirically established.

6. AUTICE Software Design

6.1 Level 1--The Main Program As indicated in Figure 6.1, the main program, AUTICE, initiates processing by calling JHR (for Julian hour which is the number of hours AFGWC's computers have been in operation) which returns the Julian hour for 0000Z or for 1200Z (whichever is more recent) for that day. Using the Julian hour, AUTICE calls TIME which uses a do-loop to execute the rest of the program. Each increment of the loop makes forecasts for the next valid time. Inside the loop, subroutine GETDAT gets the data; MTNS gets lists of points below the terrain at 850, 700, and 500 mb; VORADV computes vorticity advection; PILIFT computes pseudo-isentropic lift; FCST generates the operational forecast field to be implemented at AFGWC; and TFCST generates the temporary forecast field used in tesing, evaluation, and development of the AUTICE software.

6.2 Level 2--Subroutines Called from AUTICE

6.2.1 VORADV VORADV (Fig 6.2) receives 500 mb heights and vorticity from AUTICE. It sends the heights to GEOWND (for geostrophic wind) which returns wind components in the I and J grid directions. The I and J components and the vorticity are next sent to ADVECT (for advection) which returns the 500 mb vorticity advection to AUTICE via VORADV.

6.2.2 PILIFT PILIFT (Fig 6.2) receives temperatures and heights from AUTICE for 1000, 850, and 700 mb. The thermal advection for each level is computed using the same calls VORADV made to compute vorticity advection. Next, the advections for 1000 and 850 mb are sent to ARYAVG (for array average) which performs a simple arithmetic average. The same is next done for the 850 and 700 mb thermal advections. PILIFT next sends the wind components to WNDDIR (for wind direction) which returns the direction. Finally, PILIFT sends the averaged thermal advections and the wind directions to SPLIFT (for subordinate pseudo-isentropic lift subroutine) which returns the PILIFT forecast to AUTICE through subroutine PILIFT.

6.2.3 FCST FCST (Fig. 6.1) receives data for the six forecast criteria from AUTICE in the form of real 47 by 51 arrays. It fills a character array with asterisks and then loops through all but the outside four rings of the AFGWC octagon (i.e., the AUTICE octagon) testing at each point until a test fails (in which case a blank is assigned to the point) or until all the tests pass. If all tests pass the letter "Y" (for yes) is assigned to the point. Since FCST is to be the operational subroutine, it sends the final array of asterisks, blanks, and Y's back to AUTICE. AUTICE forwards this array to TFCST for hardcopy display.

6.2.4 TFCST TFCST is a temporary subroutine which generates the temporary forecast fields used for testing, evaluation, and development of the software. It receives the same data in real arrays that FCST receives plus the terrain fields, the whole mesh points of the Diagnostic Weather Element (DWE) icing forecast, and the array produced by FCST. TFCST then produces the maps and statistics discussed below. In the case of maps, points with the letter "M" have terrain at or above the indicated pressure level. "M" stands for mountains.

6.2.4.1 Primary Fields These are the temperature, omega, cloud, and dew-point depression fields which are used as is with no computations. At each of the three levels, TFCST prints maps with the letters "T," "O," "C," and "D" at the points meeting the criteria stipulated in paragraph 4. For illustrations of each see Fig. 6.3 to 6.6.

6.2.4.2 Lift Fields The 500 mb vorticity advection map prints "V" at points with PVA. The PILIFT map prints the letters "L" and "U" at the lower and upper level PILIFT points. A fourth map prints the letter "A" (for logical AND) at points meeting all three lift criteria. Finally, a fifth map has the letter "R" (for logical OR) at all points where one or more of the three lift criteria are met. See Figs. 4.5, 4.6, 6.7, 6.8, and 6.9 for illustrations of each.

6.2.4.3 Forecast Fields The AUTICE Map prints "Y" (for yes) at points icing is forecast for. At points where DWE forecasts icing the letter "E" is printed (for DWE). The AIDWE map is a combined AUTICE and DWE map with the letter "B" printed at points both AUTICE and DWE forecasted for, the letter "Y" at points only AUTICE forecasted for, and the letter "E" at points only DWE forecasted for. Letter counts are printed at the bottom of the map. Another map with a modified AUTICE forecast prints the letter "Y" at points having one or more forms of lift. A final map prints the number of tests passed at each point. See Figs. 6.8 and 6.10 to 6.13 for illustrations of each.

6.2.4.4 Verification Map RAOBII is the verification map on which RAOB analyzed icing is manually plotted. The letter "O" is printed over the whole mesh points in the European and conterminous United States Boundary Layer Model (CONUS BLM) windows. Scales on the top and left sides of each window indicate the last digit of the I or J. The scales will be overprinted by the letter "M" (for mountains) where mountains are present. See Fig. 4.6 for illustration.

6.2.4.5 Statistics To evaluate the degree of overlap among the six AUTICE criteria, statistical counts of the criteria met at each point are made. NBTO is the number of points for which both temperature (T) and omega (O) criteria are met. NFTO is the number of points for which the first (i.e., temperature) of the TO pair are met. Finally, NNTO is the number of points at which neither temperature nor omega criteria are met. The second two letters of the four letter variable correspond to the letters printed on the maps with the exception of the two layers of PILIFT ("U" and "L"). For PILIFT the letter "P" is used to indicate that one or both of the PILIFT criteria were met at that point. See Fig. 6.14 for an illustration. Another count display (Fig. 6.15) shows the number of criteria met at each point.

6.3 Level 3--Subroutines Called by Level 2 Subroutines This discussion will be limited to the subroutines which do the actual meteorological computations. These are the subroutines called by VORADV and PILIFT. Figs. 6.1 and 6.2 show the interrelationships between these subroutines.

6.3.1 GEOWND GEOWND uses heights from VORADV or PILIFT to compute the wind component in the I grid direction (U component) and the J grid direction (V component). These gridded U and V wind components are not to be confused with the normal convention of northerly and easterly wind components. GEOWND

loops through all but the outside ring of AFGWC octagon points computing U and V components at each point before proceeding to the next point. The looping proceeds one row at a time. At each point GEOWND converts the (I,J) coordinate for the point from integer to real format. GEOWND then sends the converted (I,J) to an AFGWC library routine which returns the latitude and longitude of the point. The latitude is used to compute both a constant based on the grid size and the Coriolis parameter. Height gradients in the I and J directions are computed. Finally, all the above parameters are inserted into (C-6) and (C-7) of Appendix C. The first equation returns the U wind component; and the second the V wind component. Appendix C gives a detailed derivation of these two formulas.

6.3.2 ADVECT ADVECT accepts U and V wind component fields and a scalar field from VORADV or PILIFT and computes the advection of the scalar field. It first intializes the 47 by 51 advection array by assigning the real number 0.0 to each point. ADVECT then loops through all but the outside two rings of the AFGWC octagon working a row at a time. At each (I,J), it calls an AFGWC library routine which returns the latitude and longitude of the (I,J). The latitude is converted to radians. A factor equal to twice the grid size at that latitude is computed. Finally, all the above parameters are inserted into an equation which returns the advection at that point. Appendix D gives a detailed derivation of the formula.

6.3.3 ARYAVG ARYAVG accepts two real 47 by 51 arrays from PILIFT. It loops through all points averaging the two values at each point. The averaged array is returned to PILIFT.

6.3.4 WNDDIR WNDDIR computes wind direction in radians measured counterclockwise from the whole mesh grid I direction. Its input consists of U and V wind components from PILIFT. WNDDIR uses the FORTRAN function ATAN (arc tangeant) which evaluates -V/U and returns the angle in radians measured counterclockwise from the I axis. This is the geometric direction convention as opposed to azimuth which would begin at the -J axis and go clockwise.

Unfortunately, ATAN is undefined for V and/or U being zero. Consequently, prior to calling ATAN, WNDDR first tests for all five undefined cases and assigns the correct angle. (For the case of U and V both being zero, the flag 7.0 is assigned.)

As with ADVECT, WNDDIR first fills the direction array with the number 0.0 and then loops through all but the outside AFGWC octagon ring going a row at a time. The direction array is then returned to PILIFT.

6.3.5 SPLIFT SPLIFT receives the averaged thermal advection for a layer and the wind directions for the bottom level of the layer from PILIFT. As with ADVECT and WNDDIR, it first assigns the number 0.0 to each point of the final array. It then loops through all but the outside four rings of the AFGWC octagon (i.e., the AUTICE octagon) going a row at a time computing PILIFT at each point.

At each point SPLIFT first tests for warm air advection. If there is none, it proceeds to the next point and allows the 0.0 to stand. If there is warm advection, SPLIFT checks the wind direction to see which of the surrounding eight points the wind most nearly blows toward. If the rate of

warm air advection at that point is less, then PILIFT is occuring at the point under consideration and 1.0 is assigned.

Upon completion, SPLIFT returns the PILIFT array to AUTICE through the subroutine PILIFT.

7. Verification/Results

7.1 Relationship of AUTICE and DWE Before examining the results or attempting any verification, it is absolutely essential to understand how AUTICE and DWE relate to one another in the context of the AFGWC models and data bases. As indicated in Fig. 7.1, PIREP, satellite, and RAOB data are stored in the AFGWC data bases and used to run the forecast models which provide data for the applications models such as DWE and AUTICE. Ultimately the applications models send their results to a high speed printer (HSP) or a data control terminal (DCT).

As pointed out in paragraph 2.3.4, NH5LYR forecasts too much moisture and cloud which when passed on to DWE result in icing being forecast for too broad of an area. As a result DWE frequently makes icing forecasts for areas that are clear by the verification hour. AUTICE is identical to DWE in that it receives the same temperature, dew-point depression, and cloud forecasts which DWE does. The similarity continues in the temperature and dew-point depression criteria. As indicated in Fig. 7.2, DWE forecasts icing in the same area TR-80 does. AUTICE differs by omitting icing in area F and by adding icing in area D. As a result AUTICE will miss icing in area F but will pick up icing (and increased false alarms) in area D. These differences are rather superficial because all models in Fig. 7.2 do forecast icing in the top left of the diagram. In the areas to the right and bottom icing frequencies fall off so that in these areas false alarms are traded off against misses depending upon the chosen cutoff point. Thus, up to this point, DWE and AUTICE are practically identical.

7.2 The AUTICE Filter Most of the differences between AUTICE and DWE are caused by AUTICE's cloud and lift filters. If DWE were converted to a Yes-No format, it would be almost identical to the AUTICE forecast prior to application of these filters. This can be verified by comparing the DWE map (Fig. 6.11) with the AUTICE map with OR'd lift criteria (Fig. 6.12). Except for the few cases where AUTICE forecasts for points in area D of Fig. 7.2 which DWE misses and the few cases where DWE forecasts for points in area F of Fig. 7.2 which AUTICE misses, the patterns are identical.

The lift filter works by requiring points which DWE and TR-80 would forecast icing for to be thrown away unless they meet the omega, PVA, and PILIFT criteria. Consequently, a point which TR-80 would forecast icing for and which had strong PVA and large omega values will be disqualified solely because it did not meet the PILIFT criterion. Just how strong this filter is may be seen in the map of points meeting the omega and vorticity and PILIFT criteria (Fig. 6.8). This map has the letter "A" printed at points where all three lift criteria are met. Thus in Fig. 7.2, I've represented the AUTICE forecast with "swiss cheese" holes to show that 95 percent of potentially qualified points are disqualified *a priori* by the lift filter.

Besides the lift filter, AUTICE has a cloud filter. The strength of this filter when added to the lift filter can be seen by overlaying the cloud map with the maps of points meeting the omega and vorticity and PILIFT criteria (Figs. 6.6 and 6.8). At 850 mb the 66 A points are reduced to 29. At 700 mb the 66 "A" points are reduced to 17. At 500 mb the 63 "A" points are reduced to 9. Averaged over all levels and recalling that there are 1491 points in the AUTICE octagon, we see that the AUTICE lift filter in conjunction with the

temperature and dew-point criteria disqualified 95.6 percent of the points and the addition of the cloud filter disqualified 98.8 percent of the points. Stated another way, the cloud filter filtered out all but 28.2 percent of the points left by the lift filter.

By contrast, DWE forecasts icing at all points meeting the temperature and dew-point criteria of TR-80. Cloud cover is used only to determine type of icing. The perception that this results in a high false alarm was not born out in the maps I examined.

Obviously the strong AUTICE filter should be relaxed. This may be done by letting it suffice to forecast icing when only one of the three lift criteria are met. The map of points meeting the omega or vorticity or PILIFT criteria (Fig. 6.9) prints the letter "R" at all points meeting one or more of the icing criteria. Unfortunately, the filter now performs like a sieve and produces a forecast which is almost identical to DWE (see Fig. 6.13).

At first glance it doesn't seem reasonable that 95 percent of the points in the Northern Hemisphere would have one or more forms of lift. Why this is so becomes more apparent when the assertion is restated, "Almost all points in the Northern Hemisphere either have vertical velocity of 1 mb hr^{-1}, or have PVA at 500 mb, or have increasing warm advection in the 1000 to 850 mb layer, or have increasing warm advection in the 850 to 700 mb layer." A quick look at Figs. 4.4, 4.5, and 6.7 shows that the last three (i.e., PVA and the PILIFTs) are the major contributors. The PILIFT fields are larger than expected because in addition to locating the warm air advection ahead of a warm front they locate warm air advection ahead of warm cores and behind cold cores.

The reason that the three lift criteria form too strong of a filter when AND'd and too weak of a filter when OR'd is contained in the point counts in Fig. 6.14. (See paragraph 6.2.4.5 for the interpretation of these figures.) In comparing the counts for vorticity, PILIFT, and omega it becomes apparent that only 20 percent of a given lift pair overlap. The remaining 80 percent don't overlap at all. When OR'd this lack of overlap increases the liklihood that one or more lift criterion will be met at a point. When AND'd, the lack of overlap makes it unlikely that all three criteria will be at any point. Figures 7.3 and 7.4 present a striking display of these overlap relationships using proportional area diagrams.

The very fact that the three forms of lift correlate so poorly with one another tends to suggest that they also cannot correlate well with icing. As mentioned previously, only an empirical study can answer that question.

7.3 Candidates for Verification Since DWE and AUTICE are virtually identical except for the filters, the only candidate for verification becomes the filter itself. Nothing is to be gained by comparing skill scores at 6, 12, 18, 24, 36, and 48 hours into the future because both are receiving the same NH5LYR input and processing it in the same manner--only the filter is different. Thus, the preferred method of verification is to verify for current data, thus avoiding the compounding of error which arises as the forecast skill for all six criteria falls off in the future. Furthermore, only the filter itself should be looked at because the AUTICE forecast is little more than DWE with a filter added. There is little to gained by

verifying the effect of the slight difference in the temperature and dew-point cutoffs since studies such as those by Thompson (1955) have already done that.

7.4 The Verification Mechanism Having identified what is different the question is, "How can we show the effect of this difference on the skill score?" How do we validate the new technique? The assumption is that the synoptic to global scale lift mechanisms produced by the models correlate with the meso-scale lift needed to counteract the glaciation rate. How do we validate that assumption? How do we prove we need 1 mb hr^{-1} vertical velocity as opposed to 5 mb hr^{-1}? What do we use as a verification mechanism?

RAOB analysis is capable only of locating cold clouds. They give little indication regarding vertical velocities on a meso-scale level. If the temperature and dew-point measurements were precise enough, frost-point analysis could be used to determine the degree of glaciation. Unfortunately that precision is not there. Hence RAOBs can't be the verification mechanism.

The problem with using PIREPs for verification have already been discussed in paragraph 1.4. AFGWC stores the PIREPs in the Regions Data Base. There is no display software to convert them into a hardcopy map which forecasters can overlay for verification purposes. Neither the Production Division nor the Resources Management Division of AFGWC verify icing forecasts in the same sense other forecasts are verified. Even though PIREPs might be suitable for operational verification of forecasts, they don't have the associated temperature, dew-point, vertical velocity, or cloud cover parameters needed to validate the AUTICE criteria or to fine-tune the placement of criteria cutoff points.

The preferred verification mechanism would be similar to the empirical verification done in the 1950's to validate the temperature, dew-point, and thermal advection criteria. An example of this may be seen in TR-80 paragraph 22.a. and Table 2 where temperature, a dew-point depression cutoff of 3° C, and thermal advection are correlated. Quoting paragraph 22.a., "Considering only the dew-point spread, there was an 84 percent probability that there would be no icing if the spread where greater than 3° C, and an 80 percent probability that there would be icing if the spread were less than or equal to 3° C." Figure 7.5 provides a graphical interpretation of this statement.

A similar study would call for aircraft reporting temperature, dew-point, vertical velocity, and cloud cover near AFGWC whole mesh points. This then would be compared with the whole mesh analysis; and a probability density curve similar to that in Fig. 7.6 would be set up for the indicated lift score or any other desired scores. My hypothetical curve indicates that the probability of icing approaches zero as subsidence becomes indefinitely large and that it approaches 100 percent as lift becomes indefinitely large.

The maximum theoretical skill of any score depends on the sharpness of the transition from low probabilities to high probabilities. If the transition is very sharp and goes from 0 percent to 100 percent probability as in Fig. 7.7, then a cutoff may be picked allowing perfect skill. There will be no false alarms, no misses. If on the other hand the curve is even flatter than in Fig. 7.6., then no matter where the cutoff is placed, the skill will be low. Hits may be increased only by moving the cutoff to the right and increasing the false alarms.

7.5 Intercorrelation With empirical verification being beyond the scope of this research, all that may be offered is an intercorrelation between RAOBII, DWE, and AUTICE which was done for 8, 9, and 13 February 1984 at 1200Z. RAOBII analyzes RAOB data for icing using the temperature and dew-point cutoffs shown in Fig 7.2. The layer meeting these criteria must be at least 2,000 feet thick for icing to be analyzed. Treating RAOBII as the ground truth, I subjectively determined that it forecast icing in 32 areas over the CONUS BLM window. The forecast was counted a hit if its area overlapped the RAOBII area. It was counted as close if its area was within one grid of the RAOBII area. Otherwise, it was counted as a false alarm and the remaining RAOBII areas were counted as misses. (The Northwest Territories of Canada were not considered.) AUTICE hit 2 areas and missed 30. It had two false alarms. By contrast, DWE hit 14 areas, was close to 7, missed 11, and had two false alarms. Maps used in the 13 February 1984 case are shown in Figs. 4.7 and 7.8. Though this does not constitute an absolute verification of either RAOBII, AUTICE, or DWE, the effect of the AUTICE cloud and lift filters was so strong that, pending verification, DWE should be the preferred model.

7.6 AUTICE in the Manual Mode The question arises as to why AUTICE, which performed so well in the manual mode has done so poorly in the automated mode? First of all, confidence in the manual technique is based on only four case studies. Thus we can't be sure the manual mode has consistently good skill. Nevertheless, having examined one of the manual technique case studies, I can suggest several reasons why the automated version would have a lower skill than the manual version.

First, the automated technique uses the coarse mesh grid points. This gives the forecaster a distinct advantage in locating patterns which cannot be resolved on the grid. This is most pronounced in locating advection patterns. The model performs linear averages (one in the I direction and one in the J direction) of the four points surrounding the point for which advection is being computed. This results in linear smoothing over a distance of 762 km at 60° N. Consequently, wherever one or more of the four surrounding grid points overlap an axis in the scalar field, anomalously low gradients will result. A similar problem occurs when the four grid points overlap an axis in the vector field. This occurs in areas of horizontal wind shear (e.g. across a pressure center or across a front) which are the very areas in which icing tends to occur. By contrast, a trained forecaster correctly infers the wind patterns in these areas (to include cross contour flow) and locates the icing. In the two case study areas, PILIFT was obvious to the forecaster but qualified by only 0.5° C in one area and was lost between the grid points in the other area.

Second, the cloud filter if used at all in the manual technique was certainly used differently. Furthermore, it would have been based on observed rather than 3DNEPH generated clouds.

Third, the automated version uses geostrophic wind as opposed to observed winds and makes no adjustments for flow around pressure centers.

Fourth, the automated version used two layers of PILIFT to filter with whereas the manual version used only the lower layer.

Fifth, not all of the parameters used in the automated version are initialized the same way in the analysis models. This probably contributes to the lack of overlap of parameters discussed in paragraph 7.2 which causes strong filtering when all parameters are required but weak filtering when only one is required.

Sixth, the forecaster knows where the front is. The model cannot resolve the front.

8. The Costs, Benefits, and Recommendations for Implementation.

8.1 The Costs

8.1.1 Implementation and Display Costs Approximately 100 programmer hours would be needed to implement AUTICE. An additional 100 hours would be needed to reduce run time and memory size. The cost to display the fields would be from 100 to 200 programmer hours. In this configuration, DWE and AUTICE would be separate models displayed on separate maps.

8.1.2 Automation Costs Once on the system AUTICE would take approximately 12 minutes 10 seconds to run on AFGWC's Sperry 1100/82. By contrast, DWE takes approximately 1 minute. Also, AUTICE would use 162 kilobytes of memory as compared with DWE's 40 kilobytes.

8.2 The Benefits

Essentially AUTICE takes the DWE forecast and filters out points. Consequently, there is no opportunity for AUTICE to locate icing DWE would be missing. (The one exception is area D of Fig. 7.2 where AUTICE locates new points at the cost of increasing false alarms.) It follows that AUTICE's major opportunity for improvement over DWE is in locating DWE points with enhanced icing potential. Whether AUTICE points do in fact have enhanced icing potential remains to be verified.

8.3 Recommendations for Implementation at AFGWC

Since DWE's advection algorithm has been empirically validated and AUTICE's filtering algorithm has not, it follows that DWE certainly should not be replaced by AUTICE. The decision to run the two models in parallel would be based on the above costs and benefits. If both the models are run, then the forecasters using them should be thoroughly briefed that AUTICE is not based on validated techniques and that it performs quite poorly if RAOBII is taken as the standard.

9. Suggested Future Research and/or Action Items

9.1 Near term at AFGWC There are several things which might be done at AFGWC in the near term at low to moderate costs. Each should be evaluated on its own merit; and its mention here should not necessarily be interpreted as an endorsement.

9.1.1 Boundary Layer Model Icing AUTICE could be modified to cover only the CONUS BLM. This would reduce both the run time and memory requirements. It might also buy an increased skill in pattern recognition.

9.1.2 3DNEPH and NH5LYR Modification 3DNEPH could be bogused over the entire globe. Condensation pressure spread curves for dew-point temperatures could be developed by latitude and season. Finally, new tuning factors could be developed to reduce the over-interpretation of clouds in the analysis.

9.1.3 PIREP Map The manual plotting of PIREPs could be automated and displayed in a 1:15 million polar stereographic projection. Although PIREPs have several weaknesses, they would provide a source of feedback to the forecasters.

9.1.4 Underlapping Fields The unexpected underlapping of the cloud and dew-point fields and of the three lift fields could be examined. Are the models being initialized differently? Is the underlap excessive?

9.1.5 Automated RAOB Overlay Technique A sister program to RAOBII using the TR-80 overlay technique described in chapter 5 could be developed.

9.2 Long Term at AFGWC

9.2.1 HIRAS/GSM Models An AUTICE model using finer mesh HIRAS/GSM data might show an increased skill in pattern recognition.

9.2.2 Verification of the Manual Technique Since the manual technique is based on only four case studies, a long term verification/interactive modification project could be undertaken. If a version with acceptable and objectively verifiable skill could be developed, then a new functional description and subsequent automation could be undertaken. However, the programmers would first observe the manual technique thus allowing them to verify that the functional description did describe the actual manual technique. Based on the programmers' evaluation of the degree to which the computer could mimic the manual technique, a go/no-go decision to automate could be made.

9.2.3 Empirical Validation An unbiased data base consisting of aircraft reported icing, temperature, dew-point depressions, and omegas at grid points and at forecast valid times could be accumulated. This could be paired with the AFGWC data bases. Using the combined data, probability density curves for the lift parameters (or any other parameters) could be developed. Model output statistics, regression analyses, and scaled forecasts could all be attempted.

9.2.4 Satellite Data Handling System Techniques SDHS's ability to combine human pattern recognition with the machine's computing ability could be exploited.

9.3 Research Outside AFGWC

9.3.1 Validation of Liquid Water Content Models The state-of-the-art is to forecast icing inferred by RAOB observed parameters. This will limit forecast skill until new parameters such as liquid water content are made available. If new liquid water content models could be developed or if current models could be validated, then that combined with the existing technology in evaluating icing penalties to airfoils could result in a quantum leap forward in icing forecast skill.

9.3.2 Drop Size Spectra Similar research in the observation and forecasting of drop size spectra could result in similar increases in forecast skill.

APPENDIX A: The AUTICE Octagon

The AFGWC whole mesh grid is a rectangular array of points overlayed on a Northern Hemispheric polar stereographic projection true at 60° N where the distance between points is 381 km. The origin point is in the top left corner with the I axis extending 47 points to the right and the J axis extending 51 points downward.

As indicated in Fig. A.1, the whole mesh octagon is simply the whole mesh grid with the corners cut off. The data accessed from the AFGWC data bases has values for each of the points in the octagon. In processing this data, each differentiation causes the border points to be lost. As a result one ring of points is lost in computing geostrophic winds from the height field (the 1's in Fig. A.1). The next ring of points is lost when wind is used to compute advection (the 2's in Fig A.1). Finally, two rings on the sides and corners and one ring on he top and bottom are lost when advection is used to compute pseudo-isentropic lift (the 3's in Fig. A.1). Thus, AUTICE forecasts are available for all but the three rings on the top and bottom and the four rings on the sides and corners. This remaining set of points (the 4's in Fig. A.1)is called the AUTICE octagon.

More information regarding AFGWC grids may be obtained from Hoke (1979).

APPENDIX B: Vertical Velocity Conversions

In order to convert mb hr^{-1} to cm s^{-1}, we must first develop a relationship between pressure and height using the hydrostatic equation:

$$dp/dz = -\rho g. \tag{B-1}$$

In the standard atmosphere from the surface to the tropopause the relationship between height in meters and temperature in Kelvins is given by:

$$T = 288.16 - 0.0065z \tag{B-2}$$

Using a surface pressure of 1013.25 mb and integrating from the surface to an indefinite level z yields:

$$z = -7726 \ln(p) + 53560 \tag{B-3}$$

where p is in millibars and z in meters. Taking the derivative of both sides of (B-3) with respect to time yields:

$$dz/dt = (-7726/p)(dp/dt) \tag{B-4}$$

where dz/dt is in mb hr^{-1}. Converting to cm s^{-1} we obtain:

$$dz/dt = (-214.6/p)(dp/dt) \tag{B-5}$$

where dz/dt is in cm s^{-1} and dp/dt is in mb hr^{-1}. Thus at 500 mb an omega of -1 mb hr^{-1} equates to an upward velocity of 0.429 cm s^{-1}. At 700 mb an omega of -1mb hr^{-1} equates to 0.307 cm s^{-1}. And at 850 mb an omega of -1 mb hr^{-1} equates to 0.252 cm s^{-1}.

(B-5) must be used with caution since it holds only below the tropopause and in a standard atmosphere.

APPENDIX C: Geostrophic Wind Algorithm

1. Introduction

Subroutine GEOWND (for geostrophic wind) receives 850, 700, and 500 mb height fields in meters from the main program AUTICE. The input field consists of AFGWC coarse mesh octagon points (see Appendix A and Fig. A.1). After receiving, the height field GEOWND uses the geostrophic wind algorithm to produce two fields of wind components in meters per second. One field consists of wind components in the direction of the grid's I axis. The other field is in the J direction. Both output fields also consist of Northern Hemispheric AFGWC coarse mesh octagon points.

At each point the geostrophic wind algorithm computes the I and J wind components in two steps:

a. First, it computes components of the height gradient in the I and J directions.

b. Second, it inserts the height gradients into the geostrophic wind equations to compute the I and J components.

2. Definitions

Z_{ij}: Height of the given pressure surface at grid point (I,J) in geopotential meters

I_g: Height gradient in the I direction

I_g: Height gradient in the J direction

ϕ: Latitude

m: Scaling factor $(1+\sin\phi)/(1+\sin 60°)$. $3.81 \times 10^5 \cdot m$ meters is the distance between grid points at latitude ϕ.

c: Magnitude of wind in natural coordinates where s is the tangential direction and n is the normal direction.

U: Wind component in grid I direction

V: Wind component in grid J direction

g: The acceleration of gravity. 9.80616 m s^{-2} will be used.

f: The Coriolis parameter expressed as $2\Omega \sin\phi = 1.4584231 \times 10^{-4} \cdot \sin\phi$ rad s^{-1}

3. Step One

In the first step height gradients in the I and J directions are computed. As illustrated in Fig C.1, the gradient components at any arbitrary point (I,J) are given by the difference between the far and near points

divided by the distance between the two points. Since the distance between any two points is 3.81×10^5 m meters, it follows that the distance between the far and near points is twice that and that:

$$I_g = (Z_{I+1,J} - Z_{I-1,J})/(2 \cdot 3.81 \times 10^5 \cdot m) \quad \text{(C-1)}$$

$$J_g = (Z_{I,J+1} - Z_{I,J-1})/(2 \cdot 3.81 \times 10^5 \cdot m) \quad \text{(C-2)}$$

4. Step Two

In the second step I_g and J_g are inserted into the geostrophic wind equation in natural coordinates given by:

$$c = -\frac{g}{f}\left(\frac{\partial z}{\partial n}\right)_p \quad \text{(C-3)}$$

where $\partial z/\partial n)_p$ is the height gradient on a constant pressure surface in the n direction which is normal (to the left) of the direction of c. Using Fig. C.2 it follows then that:

$$U = (g/f)\, J_g \quad \text{(C-4)}$$

$$V = -(g/f)\, I_g \quad \text{(C-5)}$$

substituting (C-1) and (C-2) into (C-4) and (C-5) and using the defined values for g,f, and m yields, upon simplification,

$$U = 0.16465617\ (Z_{I,J+1} - Z_{I,J-1})/(\sin\phi + \sin^2\phi) \quad \text{(C-6)}$$

and

$$V = -0.16465617\ (Z_{I,J+1} - Z_{I,J-1})/(\sin\phi + \sin^2\phi) \quad \text{(C-7)}$$

which are the geostrophic wind equations used in GEOWND.

APPENDIX D: Advection Algorithm

1. Definitions

$\vec{V}_{IJ}$: Wind velocity at point (I,J)

U_{IJ}: Component of wind in I direction at point (I,J)

V_{IJ}: Component of wind in J direction at point (I,J)

∇S_{IJ}: Gradient of scalar field at point (I,J)

I_g: Component of ∇S_{IJ} in I direction

I_g: Component of ∇S_{IJ} in J direction

S_{IJ}: Value of scalar field S at point (I,J)

ϕ_{IJ}: latitude at point (I,J)

m_{IJ}: Polar stereographic scaling factor at point (I,J) equal to $(1+\sin\phi)/(1+\sin 60°)$ for the AFGWC Northern Hemispheric whole mesh octagon. The distance between gridpoints at (I,J) is 3.81×10^5 m meters.

2. Classical Equation

The classical equation of advection at point (I,J) is

$$-(U_{IJ},V_{IJ}) \cdot (I_g, J_g) = -U_{IJ}I_g - V_{IJ}J_g. \qquad \text{(D-1)}$$

From Appendix C paragraph 3 we may expand I_g and J_g and get

$$-(U_{IJ}(S_{I+1,J} - S_{I-1,J})/(2\ 3.81\times10^5 \text{ m}) \\ -V_{IJ}(S_{I,J+1}-S_{I,J-1})/2\ 3.81\times10^5 \text{m}) \qquad \text{(D-2)}$$

In subroutine ADVECT the equivalent form

$$-(U_{IJ}(S_{I+1,J} - S_{I-1,J}) + V_{IJ}(S_{I,J+1} - S_{I,J-1}))/408354.6(1+\sin\phi) \qquad \text{(D-3)}$$

is used.

APPENDIX D: Advection Algorithm

1. Definitions

$\vec{V}_{IJ}$: Wind velocity at point (I,J)

U_{IJ}: Component of wind in I direction at point (I,J)

V_{IJ}: Component of wind in J direction at point (I,J)

∇S_{IJ}: Gradient of scalar field at point (I,J)

I_g: Component of ∇S_{IJ} in I direction

I_g: Component of ∇S_{IJ} in J direction

S_{IJ}: Value of scalar field S at point (I,J)

ϕ_{IJ}: latitude at point (I,J)

m_{IJ}: Polar stereographic scaling factor at point (I,J) equal to $(1+\sin\phi)/(1+\sin 60°)$ for the AFGWC Northern Hemispheric whole mesh octagon. The distance between gridpoints at (I,J) is $3.81 \times 10^5 \cdot m$ meters.

2. Classical Equation

The classical equation of advection at point (I,J) is

$$-(U_{IJ},V_{IJ}) \cdot (I_g, J_g) = -U_{IJ}I_g - V_{IJ}J_g. \qquad \text{(D-1)}$$

From Appendix C paragraph 3 we may expand I_g and J_g and get

$$-(U_{IJ}(S_{I+1,J} - S_{I-1,J})/(2\ 3.81\times10^5 \cdot m) \\ -V_{IJ}(S_{I,J+1}-S_{I,J-1})/2\ 3.81\times10^5 m) \qquad \text{(D-2)}$$

In subroutine ADVECT the equivalent form

$$-(U_{IJ}(S_{I+1,J} - S_{I-1,J}) + V_{IJ}(S_{I,J+1} - S_{I,J-1}))/408354.6(1+\sin\phi) \qquad \text{(D-3)}$$

is used.

REFERENCES

_____, 1979: The Use of the Skew T, Log P Diagram in Analysis and Forecasting, Air Weather Service, Scott AFB IL, Report No. AWS/TR-79/006, 145 pp.

_____, 1980: Forecasters' Guide on Aircraft Icing, Air Weather Service, Scott AFB IL, Report No. AWS/TR-80/001, 61 pp.

_____, 1981: Aircraft Icing Avoidance and Protection, National Transportation Safety Board, Washington, DC, Report No. NTSB-SR-81-1, 16 pp.

Feddes, Robert G., 1974: A Synoptic-Scale Model for Simulating Condensed Atmospheric Moisture, USAF Environmental Technical Applications Center, Washington, DC, Report No. USAFETAC TN 74-4. 21pp.

Heymsfield, 1975: Measurements and Predictions of Precipitation Development in Stratiform Ice Clouds, Meteorology Research Inc, Altadena CA, Report No. AFCRLTR-75-0564, 88pp.

Hobbs, Peter V., 1980a: Studies of Extratropical Cyclonic Storms (The CYCLES Project), Department of Atmospheric Sciences, Washington University, Seattle WA, Report No. AFOSR/TR-80/1279, 9pp.

Hobbs, P. V., T. J. Matejka, P. H. Herzegh, J. D. Locatelli, and R. A. Houze, Jr., 1980b: The Mesoscale and Microscale Structure and Organization of Clouds and Precipitation in Mid-latitude Cyclones. I: A Case Study of a Cold Front, J. Atmos, Sci., 37pp, 568-596.

Hoke, James E., J. L. Hayes, and L. G. Renninger, 1979: Map Projections and Grid Systems for Meteorological Applications, Air Force Global Weather Central, Offutt AFB NE, Report No. AFGWC/TN-79/003, 86 + xii pp.

Peirce, R. M., R. W. Lenhard, and B. F. Wiess, 1975: Comparison Study of Models Used to Prescribe Hydrometer Water Content Values, Part I: Preliminary Results, Air Force Cambridge Research Laboratories, Bedford, MA, Report No. AFCRL-TR-75-0470, 14pp.

Rapp, R. R., 1979: Aircraft Icing During Low-level Flights. Rand, Santa Monica, CA, 14pp.

Riehl, H. and Reinking, R. F., 1981: Study of an "Upslope" Snowstorm, National Oceanic and Atmospheric Administration, Environmental Research Labs, Boulder, CO, Report No. TM ERL WMPO-44, 30pp.

Thompson, J. K., 1955: 1954 Icing Presentation for Major Commands, Wright Air Development Center, Report No. WCT 55-26.

Touart, Chankey N. and Utaka Izumi, 1979: Comparison Study of Models Used to Prescribe Hydrometer Water Content Values, Part II: USSR Date, Air Force Geophysics Laboratory, Hanscom AFB MA, Report No. AFGL-TR-79-0213, 51pp.

Wallace, John M. and Peter V. Hobbs, 1977: Atmospheric Science an Introductory Survey, Academic Press, New York, 467pp.

Whiton, Roger C., 1984: Personal communication.

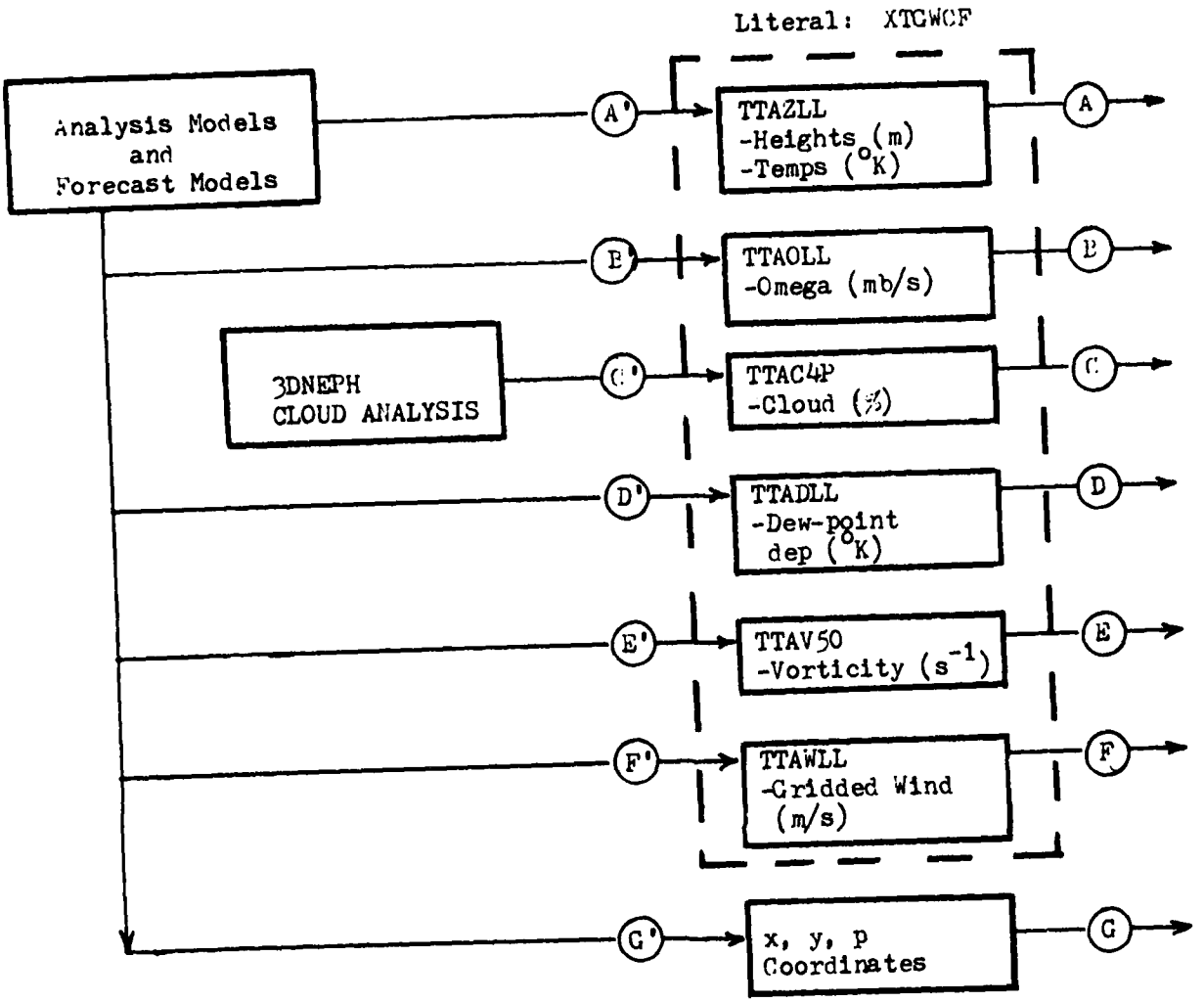

Figure 2.1 The flow of data and its processing as related to the creation of both the present DWE icing forecast and the proposed automated icing forecast (AUTICE). To simplify the diagram, only the whole mesh literal has been drawn. Fig. 2.2 is a continuation.

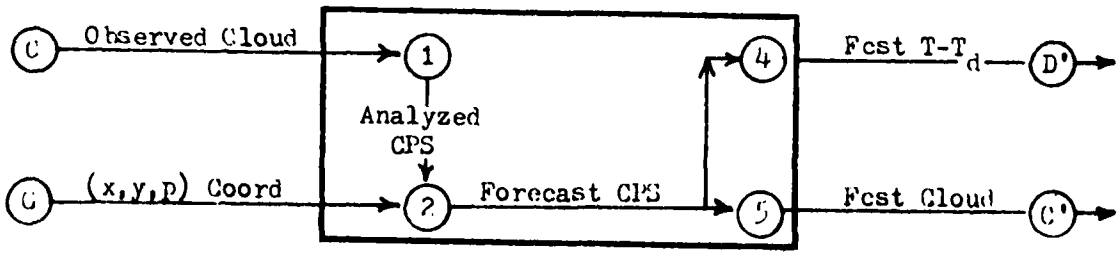

NH5LYR MODEL

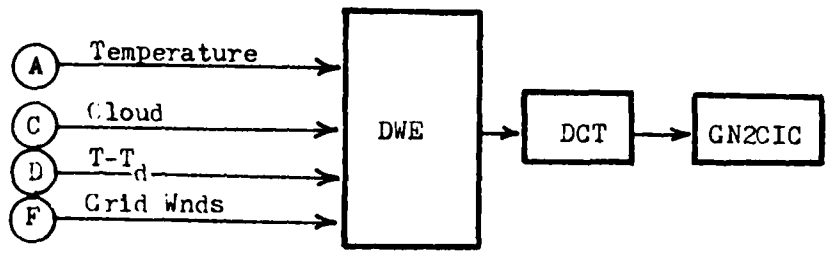

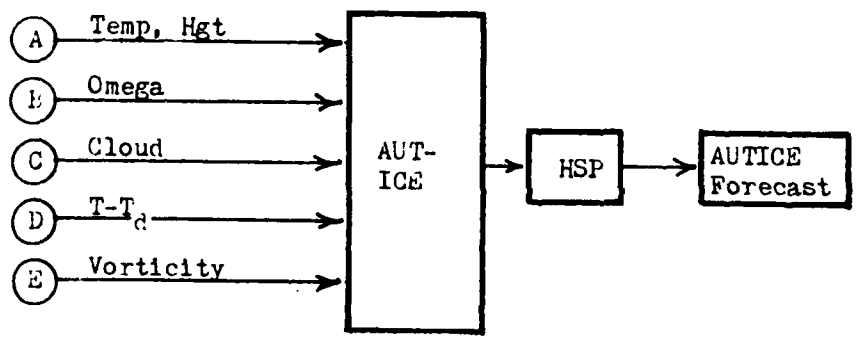

Figure 2.2 Continuation of Fig 2.1 showing the flow of data and its processing as related to the creation of both the present DWE icing forecast and the proposed Automated Icing forecast (AUTICE). To simplify the diagram, only whole mesh data is depicted.

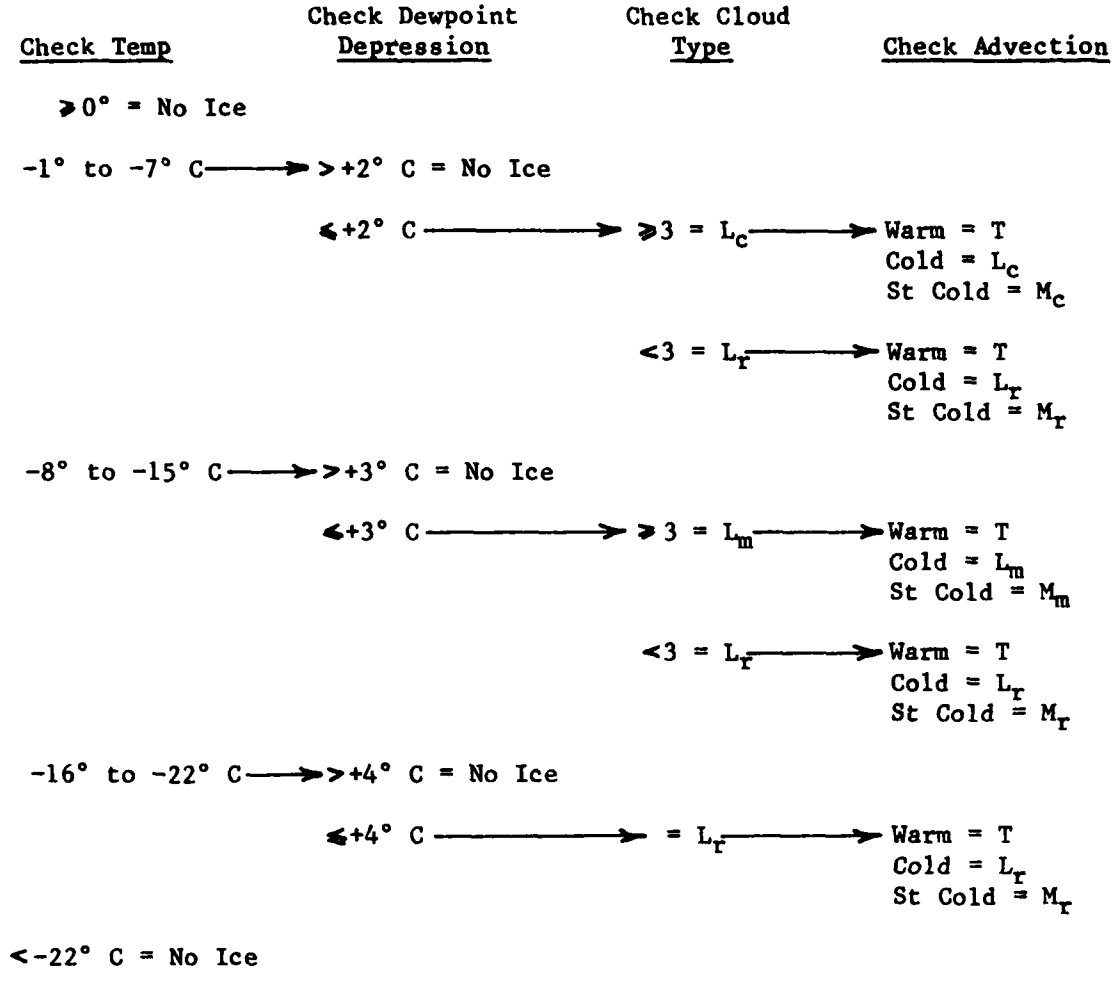

Figure 2.3 Diagnostic Weather Elements Icing Forecast Flow Diagram. Cloud type 1 is stratus, 2 is mixed, 3 is cumulus, 4 is towering Cu, and 5 is CB. Icing intensity T is trace, L is light, and M is moderate. Icing type r is rime, m is mixed, and c is clear. Warm advection is ≥ -0.1° C, cold is < -0.1° C to ≥ -2° C, and strong cold is < -2° C.

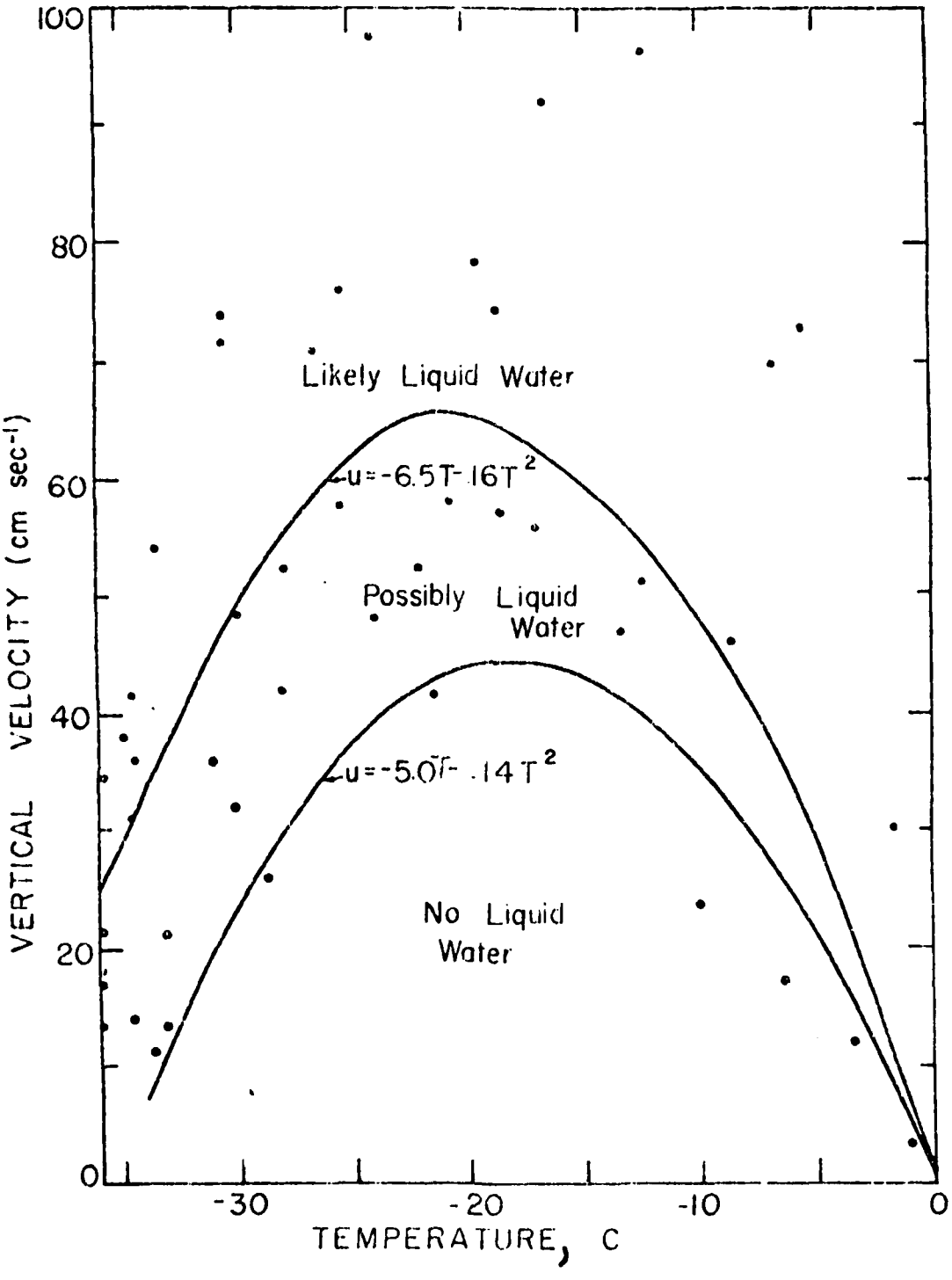

Figure 4.1 Criteria for liquid water to occur in stratiform ice clouds. Data points: Calculated air velocity necessary for liquid water to occur. Lower line: Below which liquid water is unlikely to occur. Upper line: Above which liquid water is likely to occur. Diagram applicable to clouds with cloud-top temperatures lower than -20°C. After Heymsfield (1975).

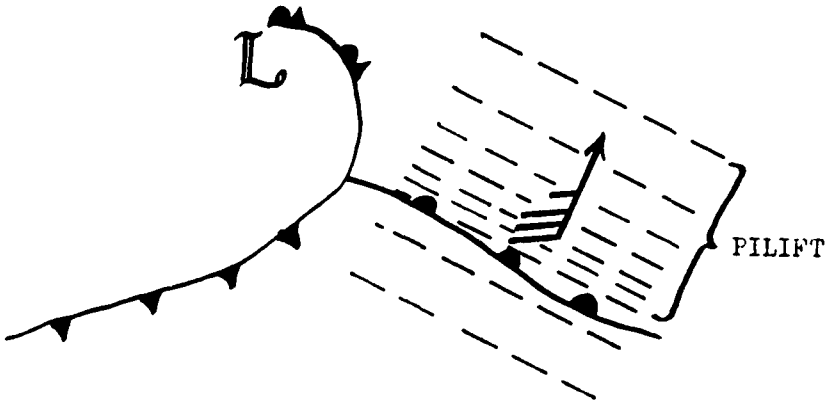

Figure 4.2 Areas pseudo-isentropic lift (PILIFT) was designed to locate.

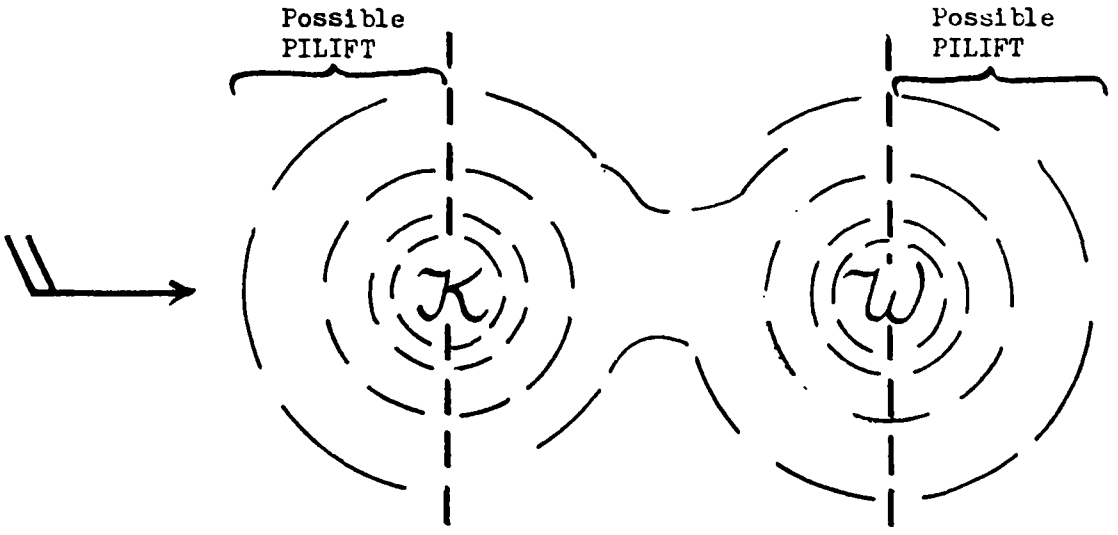

Figure 4.3 It is possible for unintended areas of PILIFT to occur with warm (W) and cold (K) thermal cores advected by the upper air flow. In this particular diagram the thermal gradient is stronger toward the center of the cores so that PILIFT occurs only ahead of the warm core. A reversed thermal gradient would cause PILIFT behind the cold core.

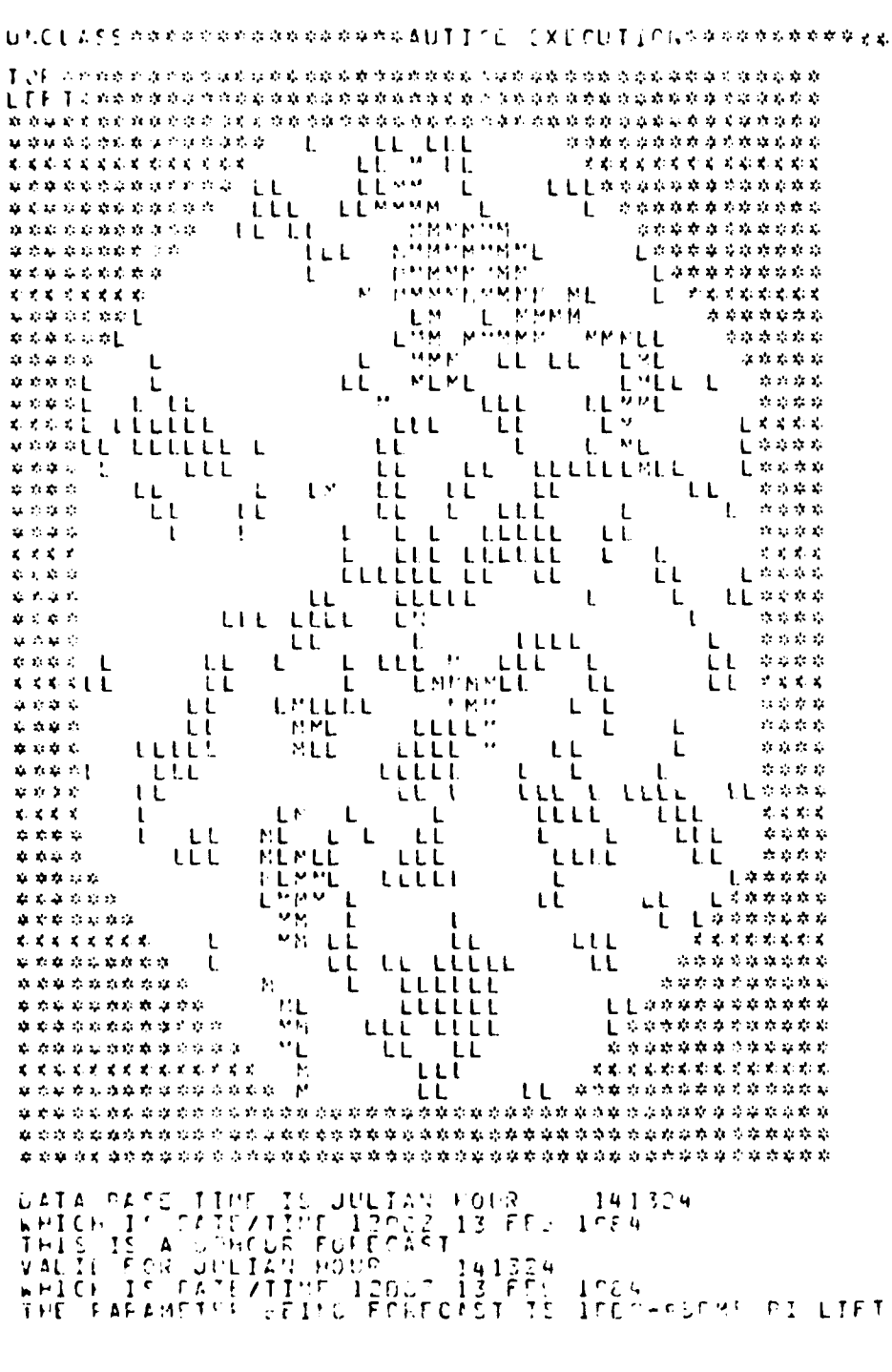

DATA BASE TIME IS JULIAN HOUR 141324
WHICH IS DATE/TIME 12002 13 FEB 1984
THIS IS A 3-HOUR FORECAST
VALID FOR JULIAN HOUR 141324
WHICH IS DATE/TIME 12002 13 FEB 1984
THE PARAMETER BEING FORECAST IS PSEUDO-ISENTROPIC LIFT

Figure 4.4 1000 to 850mb Pseudo-Isentropic Lift

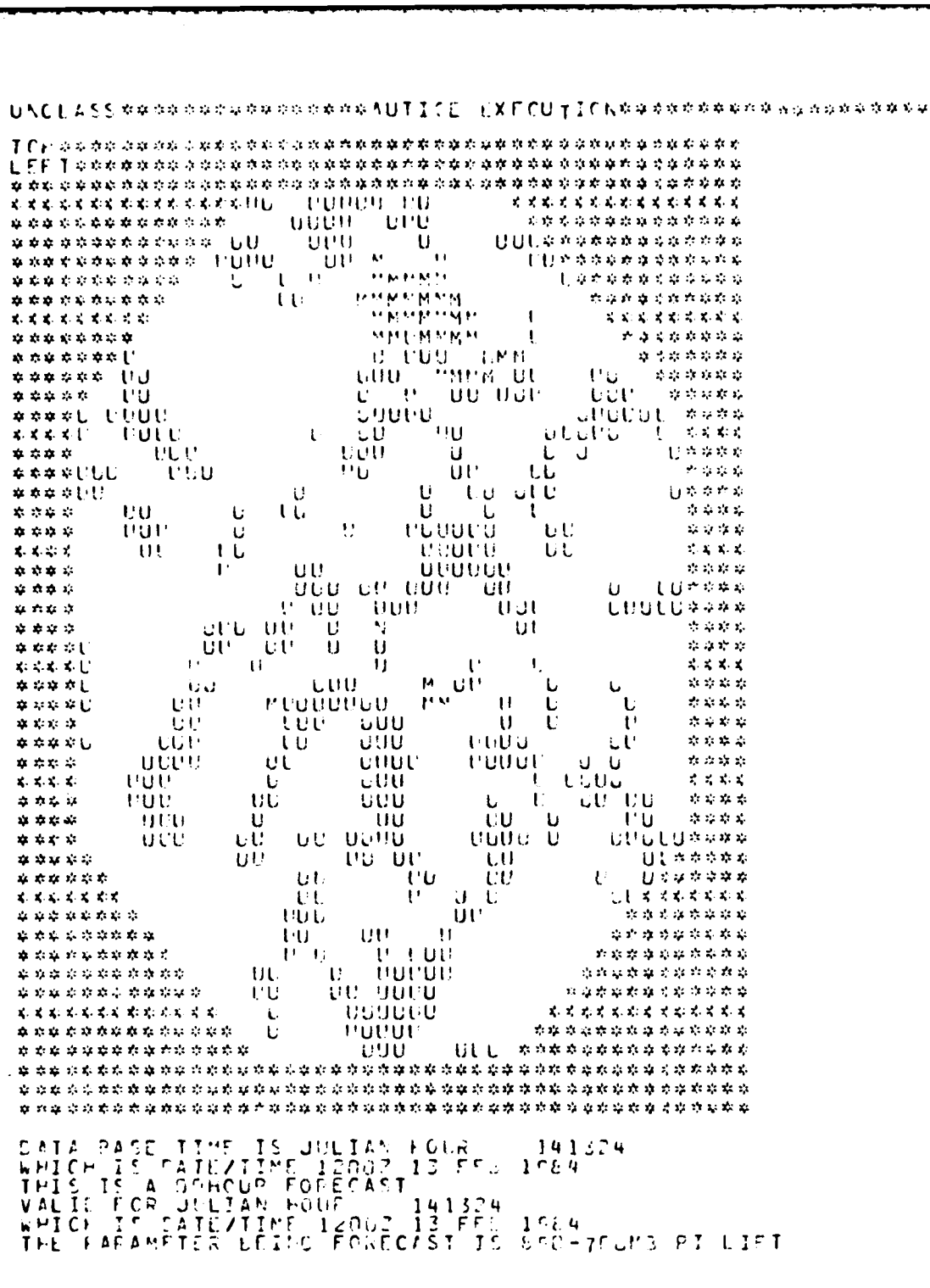

DATA BASE TIME IS JULIAN HOUR 141324
WHICH IS DATE/TIME 12002 13 FEB 1984
THIS IS A 00HOUR FORECAST
VALID FOR JULIAN HOUR 141324
WHICH IS DATE/TIME 12002 13 FEB 1984
THE PARAMETER BEING FORECAST IS 850-700MB PI LIFT

Figure 4.5 850 to 700mb Pseudo-Isentropic Lift

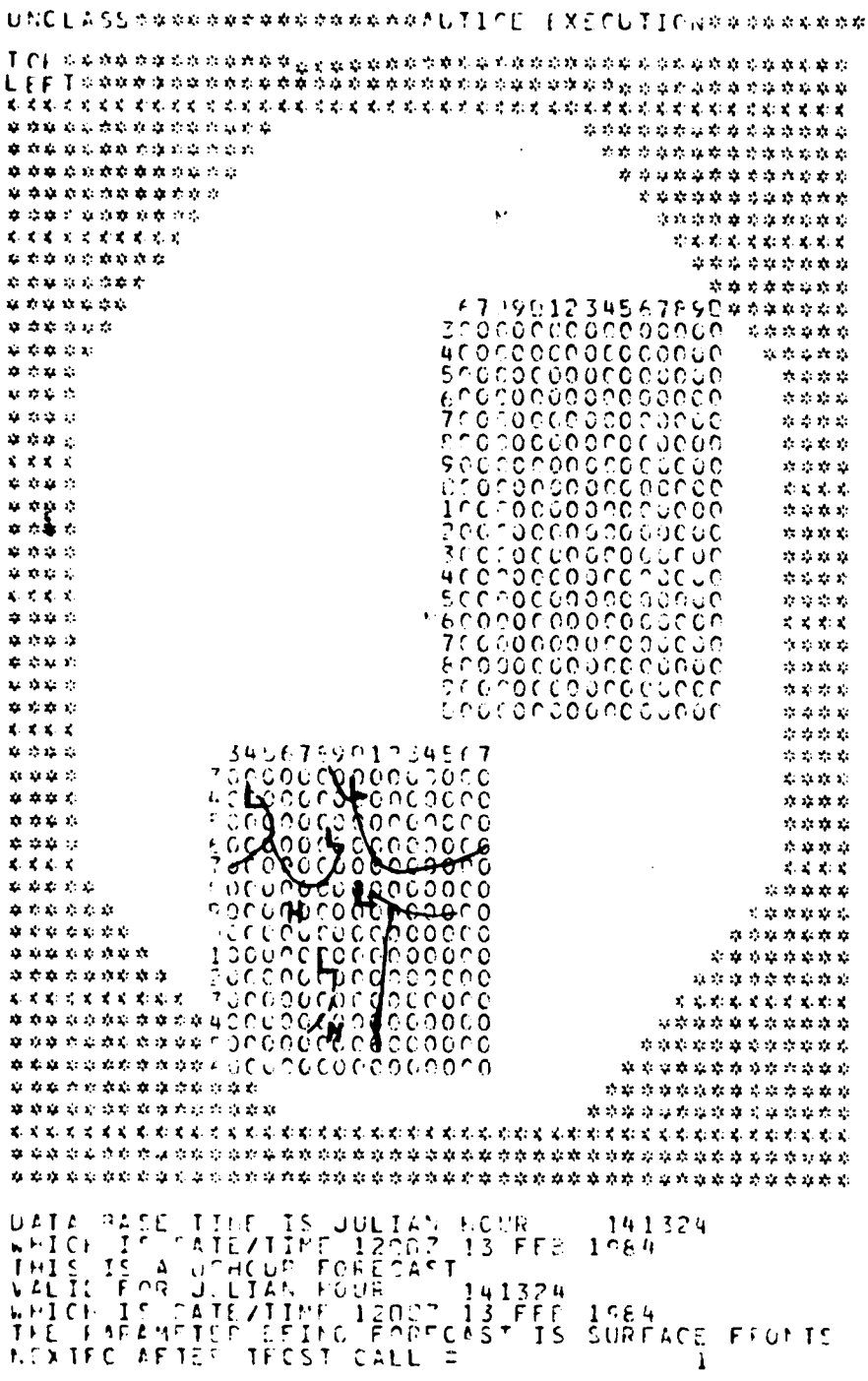

Figure 4.6 Surface Fronts in CONUS BLM

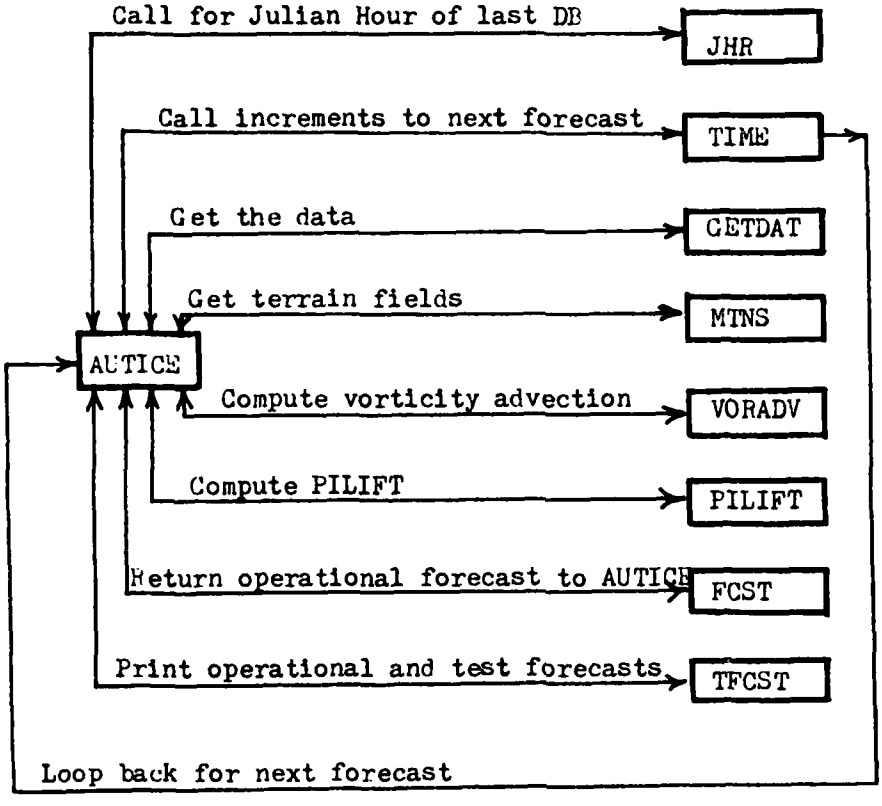

Figure 6.1 Levels 1 and 2 of the AUTICE software design. See paragraphs 6.1 and 6.2 for details.

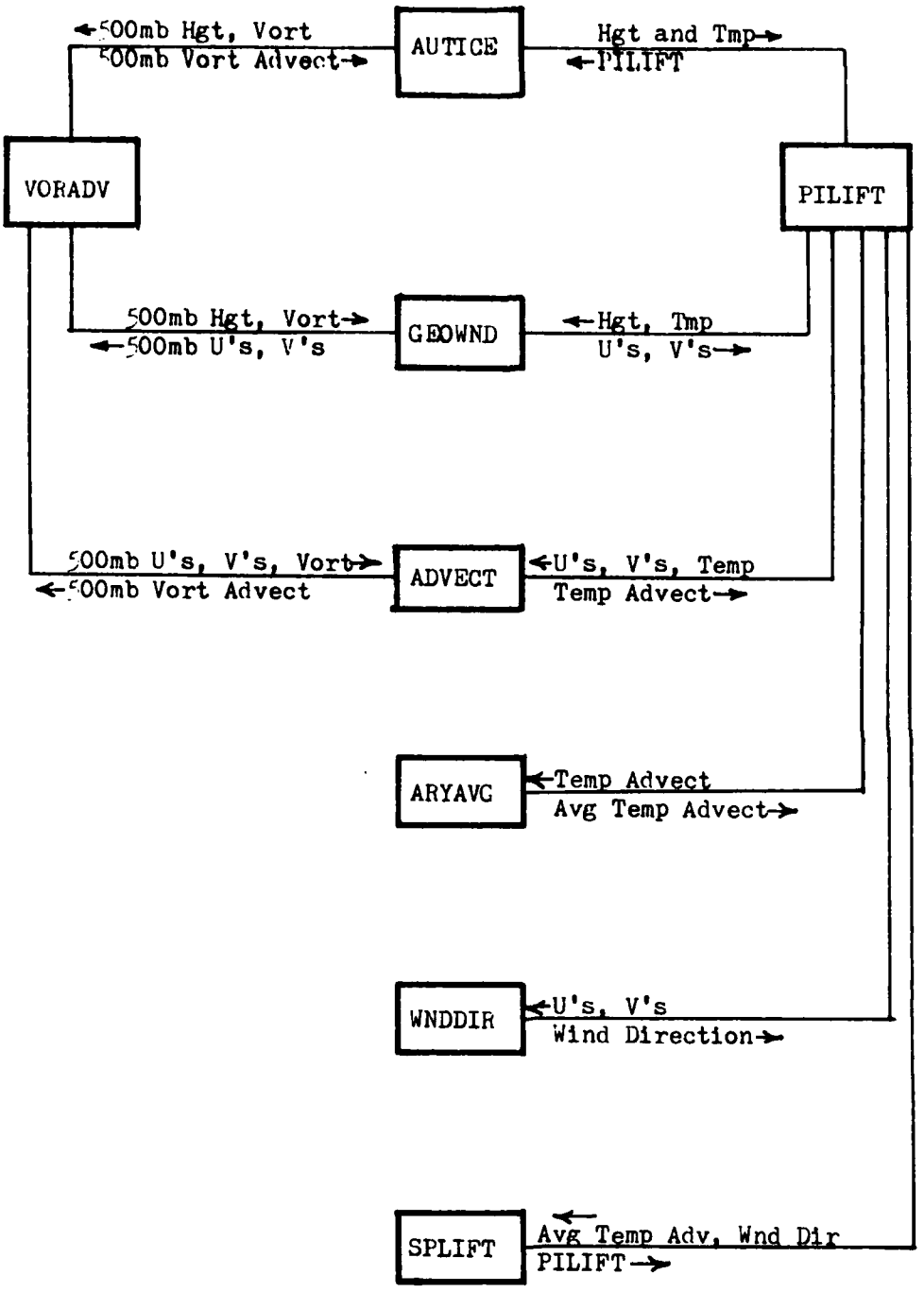

Figure 6.2 Level 2 subroutines used to compute vorticity advection and PILIFT. See paragraphs 6.2 and 6.3 for details.

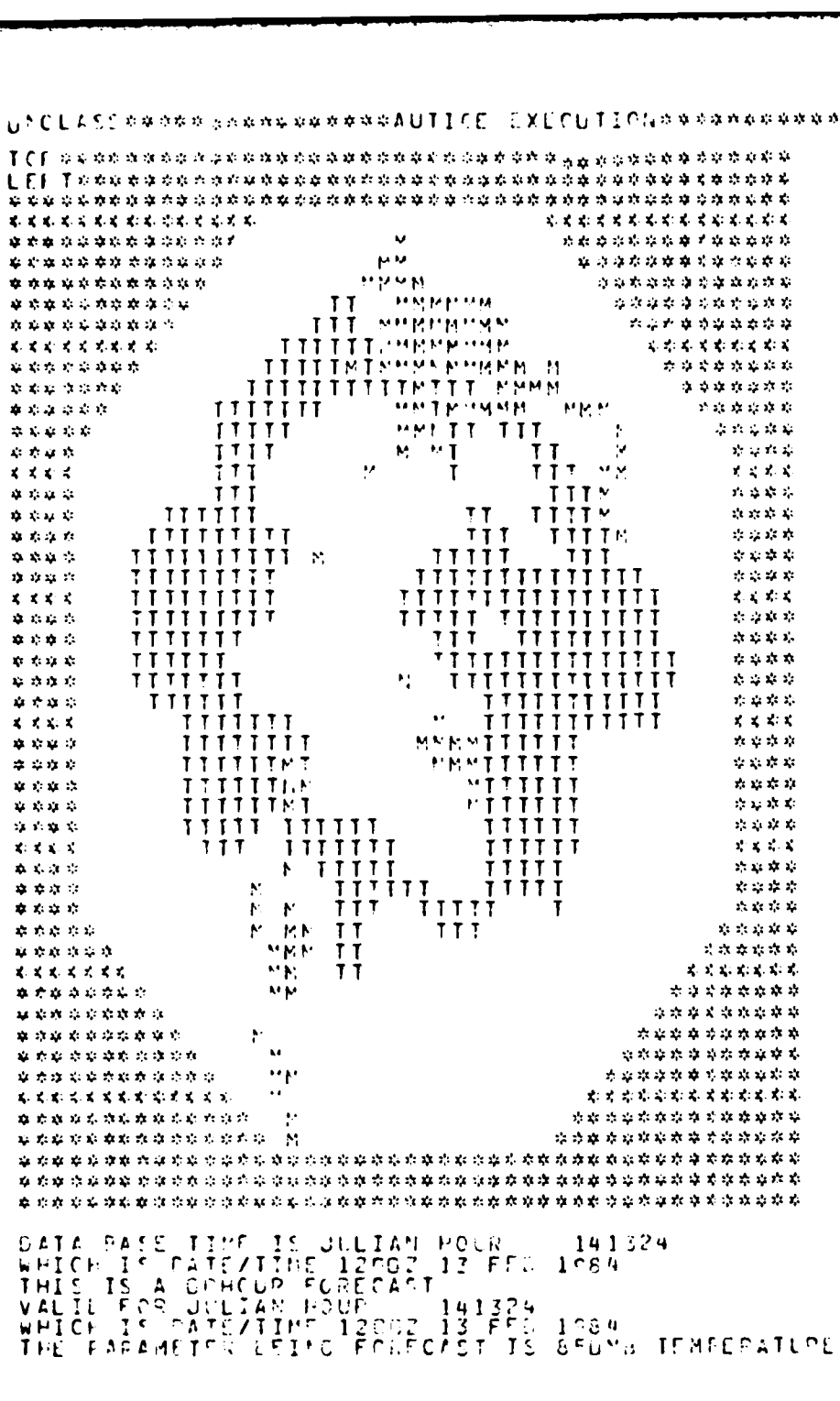

Figure 6.3 850mb Temperature

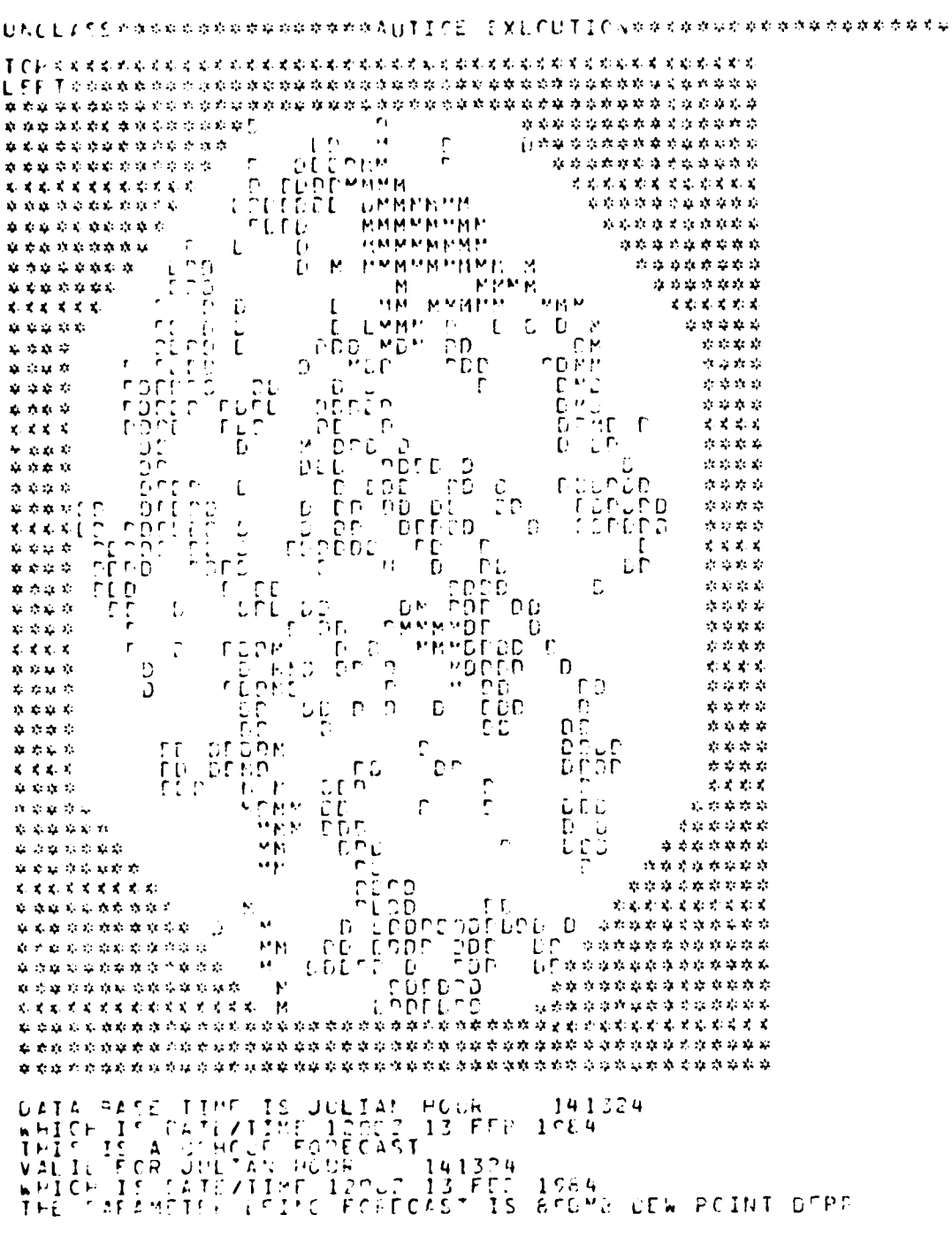

Figure 6.4 850mb Dew-Point Depression

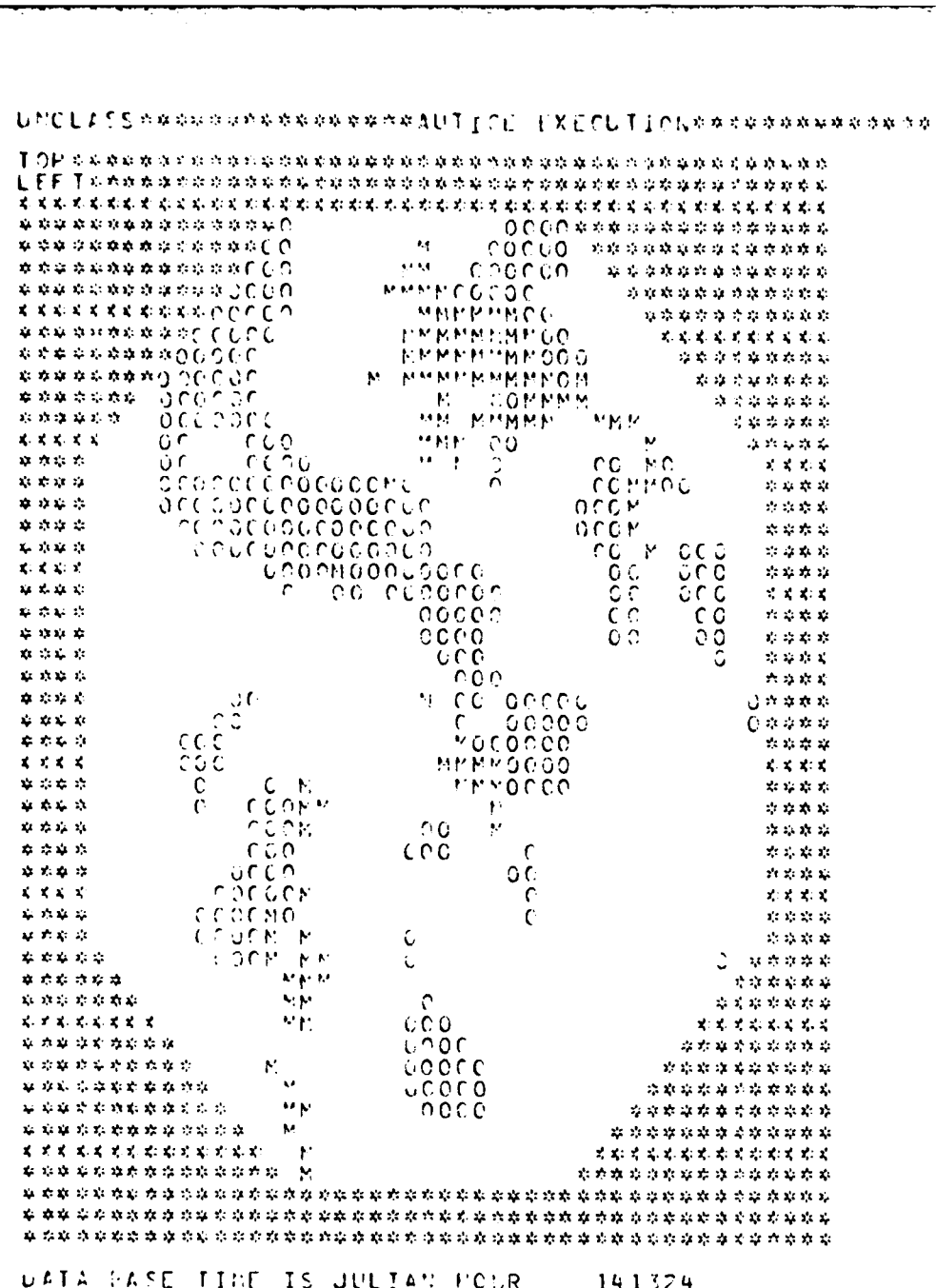

Figure 6.5 850mb Vertical Velocity (Omega)

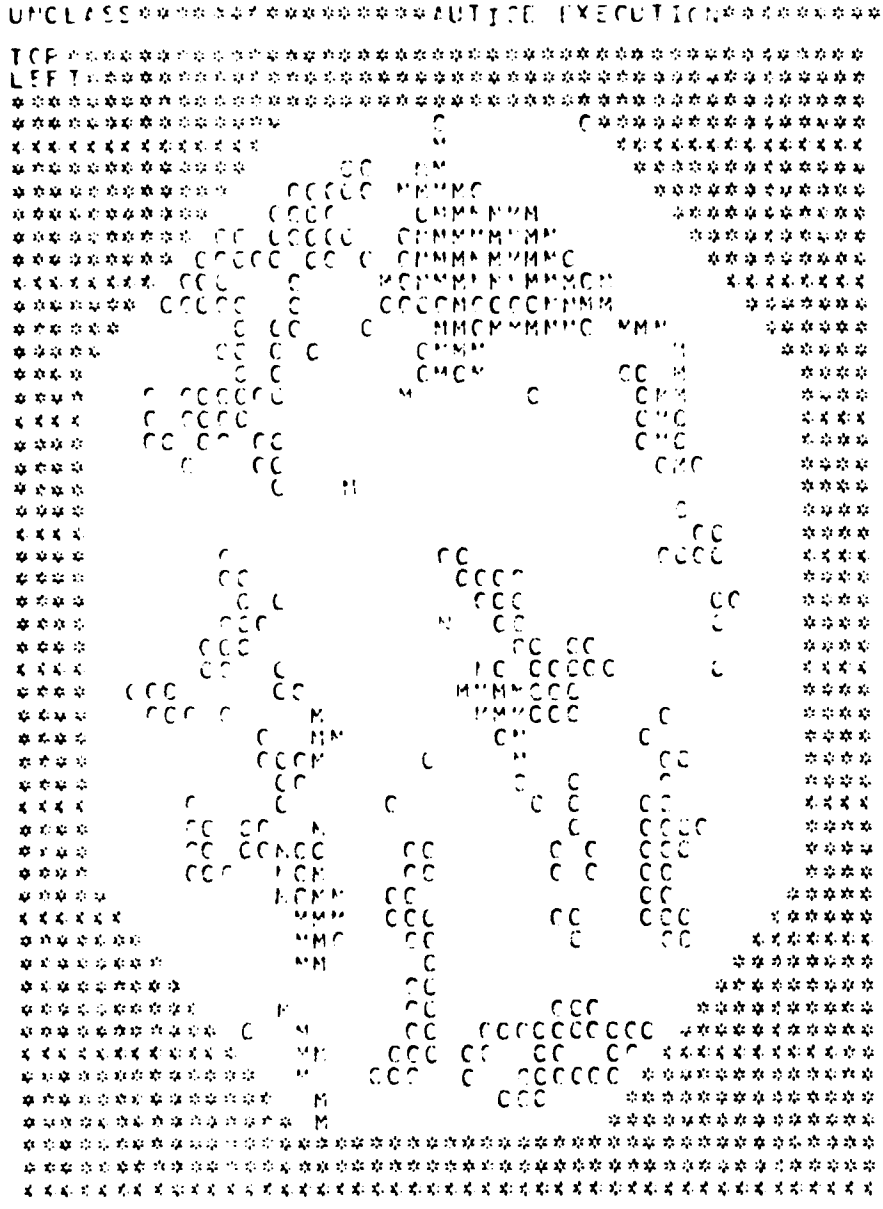

DATA BASE TIME IS JULIAN HOUR 141324
WHICH IS DATE/TIME 12007 13 FEB 1984
THIS IS A SPECIAL FORECAST
VALID FOR JULIAN HOUR 141324
WHICH IS DATE/TIME 12007 13 FEB 1984
THE PARAMETER PLOTTED FORECAST IS SECND CLOUD

Figure 6.6 850mb Clouds

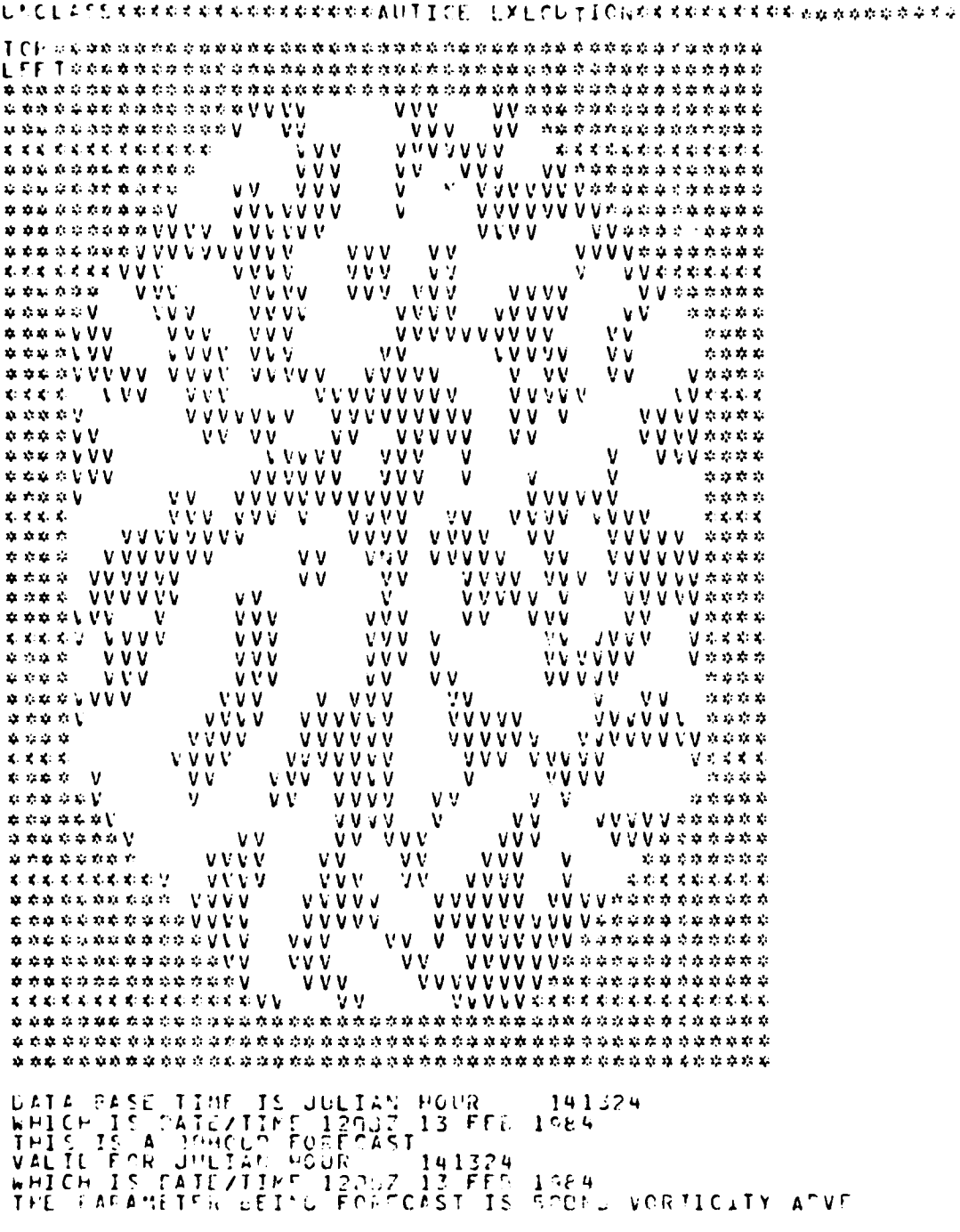

Figure 6.7 500mb Vorticity Advection

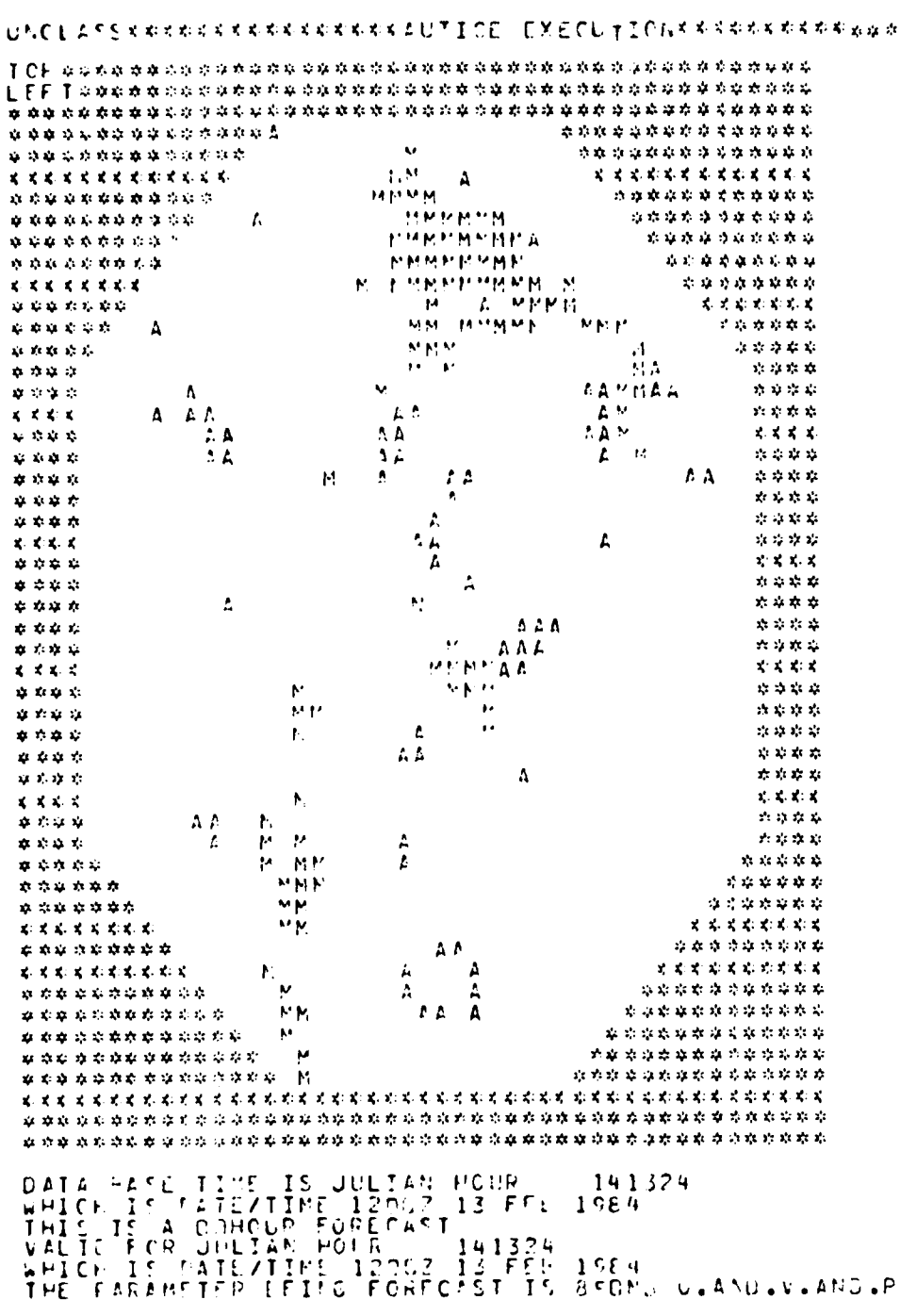

DATA BASE TIME IS JULIAN HOUR 141324
WHICH IS DATE/TIME 1200Z 13 FEB 1984
THIS IS A 00HOUR FORECAST
VALID FOR JULIAN HOUR 141324
WHICH IS DATE/TIME 1200Z 13 FEB 1984
THE PARAMETER FIELD FORECAST IS SIGMA O.AND.V.AND.P

Figure 6.8 Points Meeting Omega and Vorticity and PI-LIFT Criteria. The letter "A" appears at points meeting all three lift criteria (viz., omega, vorticity, and PILIFT).

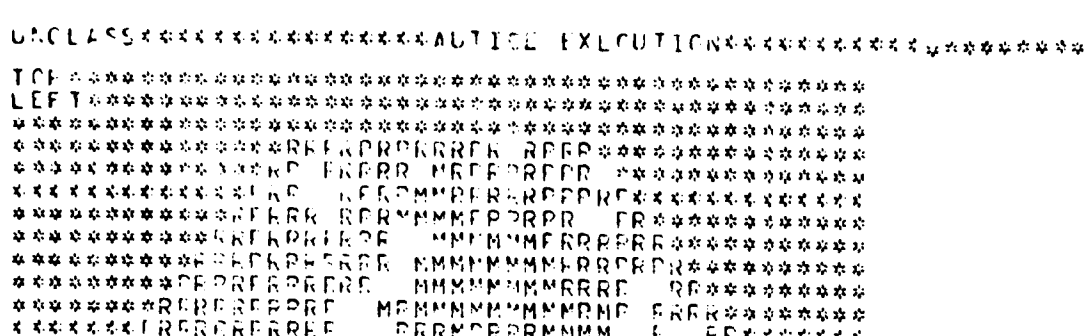

DATA BASE TIME IS JULIAN HOUR 141324
WHICH IS DATE/TIME 12007 13 FEB 1984
THIS IS A 06HOUR FORECAST
VALID FOR JULIAN HOUR 141324
WHICH IS DATE/TIME 12007 13 FEB 1984
THE PARAMETER BEING FORECAST IS BECMB U.O%.V.CF.P

Figure 6.9 Points Meeting Omega or Vorticity or PILIFT Criteria. The letter "R" appears at points meeting one or more of the three lift criteria (viz., omega, or vorticity, or PILIFT).

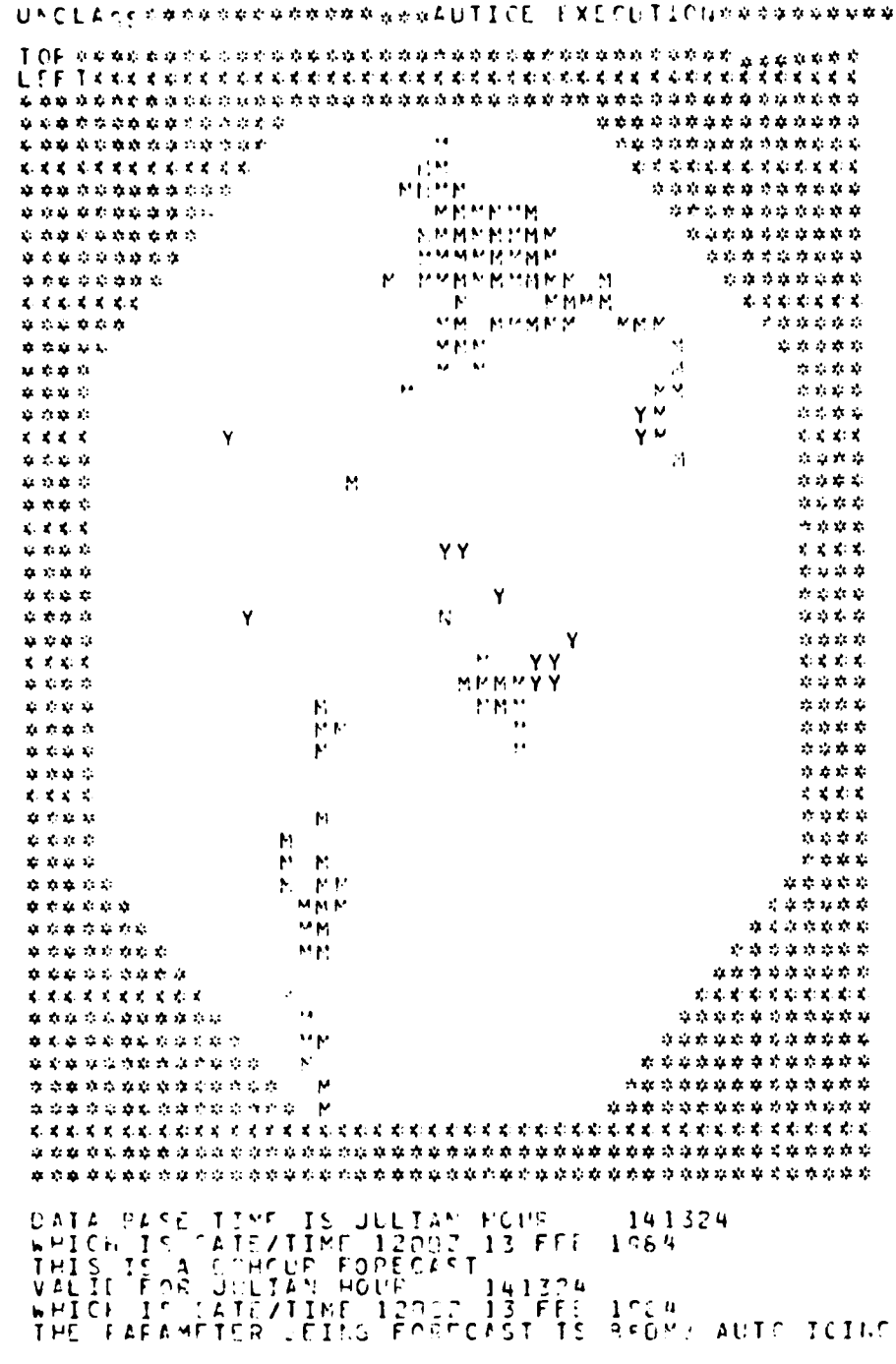

Figure 6.10 Automated Icing (AUTICE) Forecast Map.

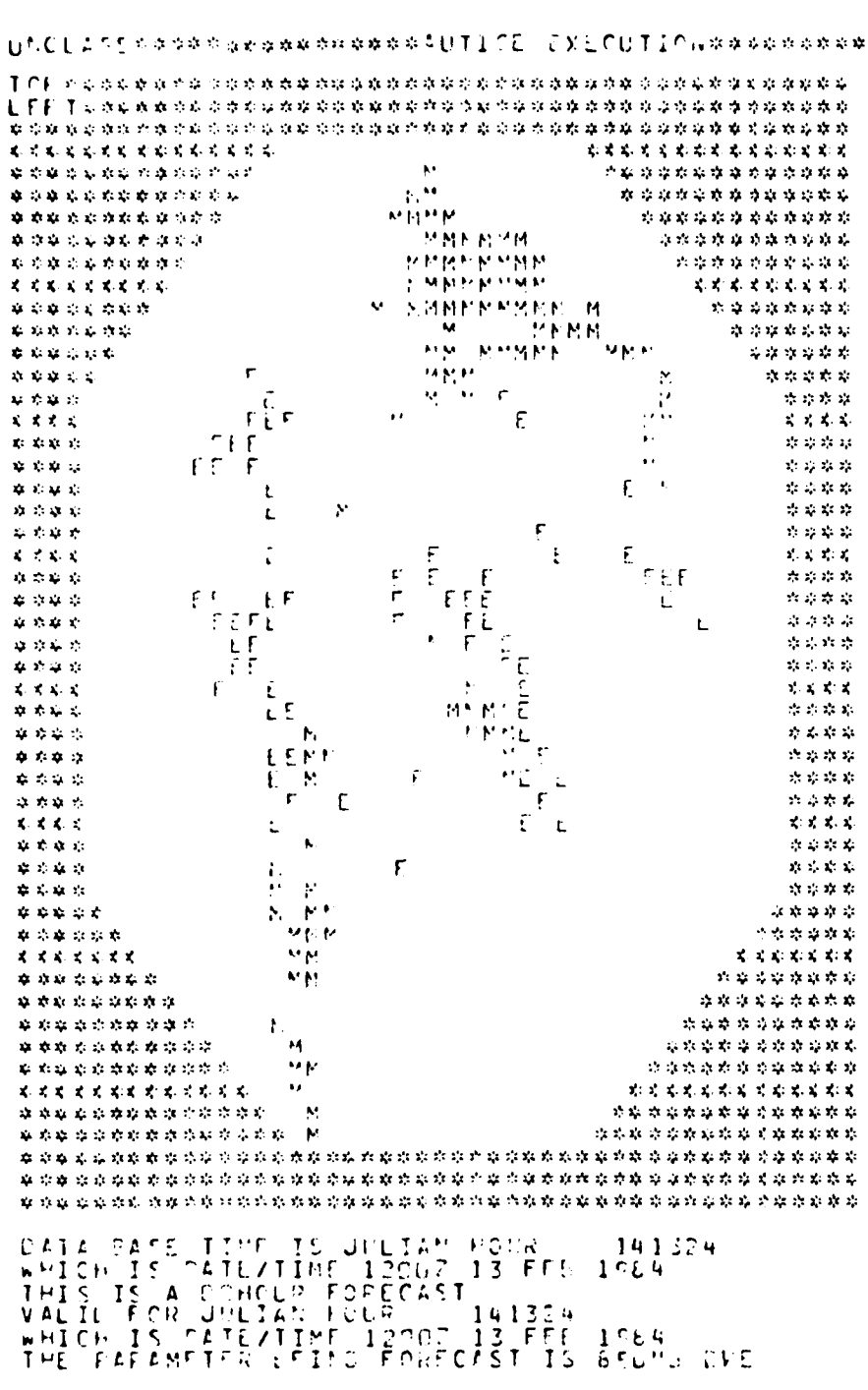

Figure 6.11 Diagnostic Weather Element (DWE) Icing Forecast Map with only whole mesh points included.

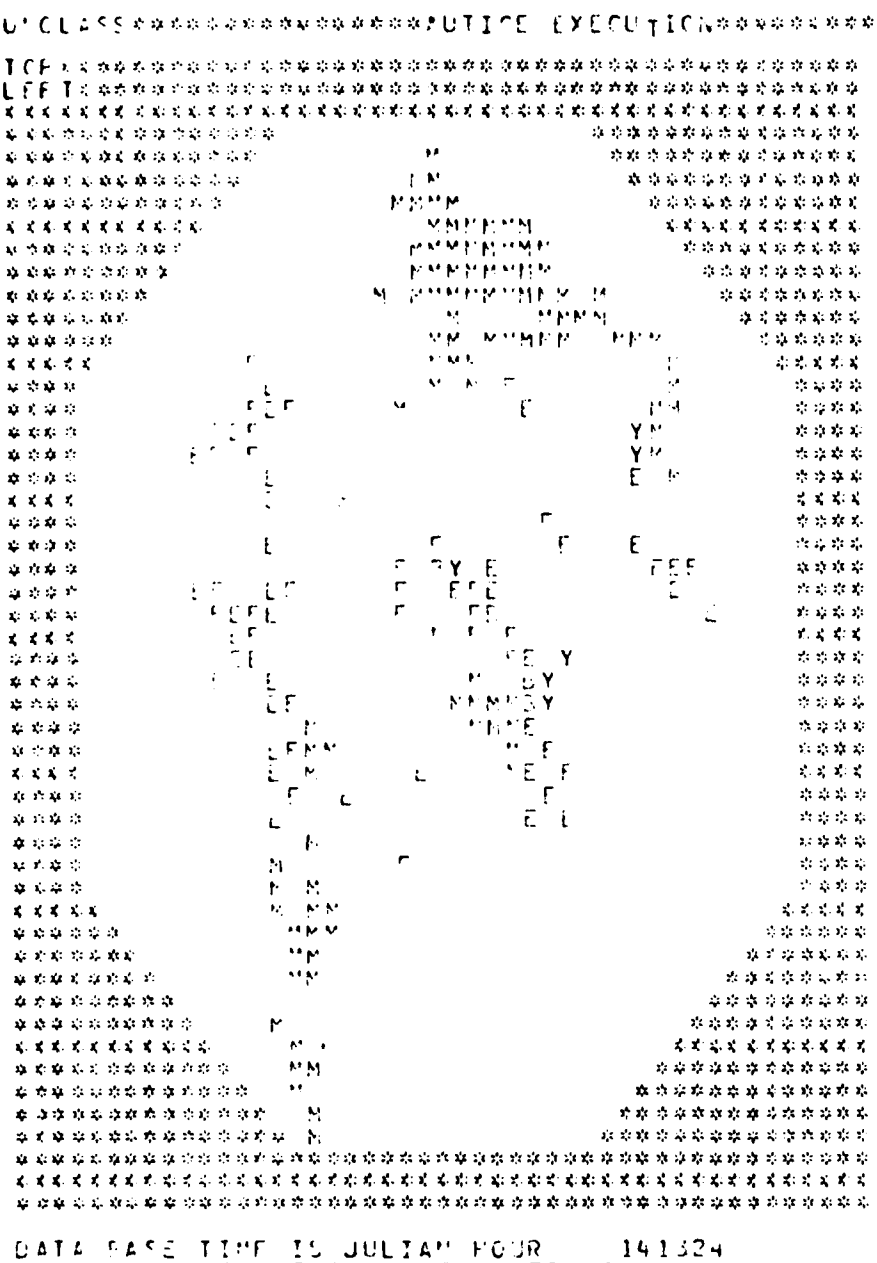

```
DATA BASE TIME IS JULIAN HOUR     141324
WHICH IS DATE/TIME 1200Z 13 FEB 1984
THIS IS A CONTOUR FORECAST
VALID FOR JULIAN HOUR     141324
WHICH IS DATE/TIME 1200Z 13 FEB 1984
THE PARAMETER BEING FORECAST IS BROMLEY
THE NUMBER OF E POINTS =     6
THE NUMBER OF E POINTS =    47
THE NUMBER OF Y POINTS =     6
```

Figure 6.12 Combined AUTICE and DWE Forecasts.

Figure 6.13 AUTICE Forecast with OR'd Lift. The letter "Y" is printed at all points AUTICE would forecast icing for if only one (or more) of the three lift criteria needed to be met to forecast icing.

UNCLASS**********AUTICE EXECUTION**********

```
8EC ML  COUNTS OF BOTH, FIRST, SECOND, NEITHER
  NB TC  =              125
  NB TC  =              118
  NB TL  =              169
  NB TV  =              228
  NB TF  =              166
  NB OC  =              132
  NB OL  =              163
  NB OV  =              195
  NB OF  =              153
  NB CL  =              202
  NB CV  =              199
  NB CF  =              141
  NB LV  =              248
  NB LF  =              206
  NB VF  =              265
  NF TC  =              297
  NF TC  =              304
  NF TL  =              253
  NF TV  =              194
  NF TF  =              256
  NF OC  =              233
  NF OL  =              202
  NF OV  =              178
  NF OF  =              212
  NF CL  =              153
  NF CV  =              156
  NF CF  =              214
  NF LV  =              216
  NF LF  =              258
  NF VF  =              504
  NS TC  =              240
  NS TC  =              237
  NS TL  =              295
  NS TV  =              541
  NS TF  =              431
  NS C   =              223
  NS CL  =              301
  NS OV  =              574
  NS OF  =              444
  NS CL  =              362
  NS CV  =              570
  NS CF  =              456
  NS LV  =              521
  NS LF  =              391
  NS VF  =              332
  NN TC  =              429
  NN TC  =              832
  NN TL  =              774
  NN TV  =              526
  NN TF  =              638
  NN OC  =              903
  NN OL  =              825
  NN OV  =              552
  NN OF  =              682
  NN CL  =              674
  NN CV  =              566
  NN CF  =              680
  NN LV  =              506
  NN LF  =              636
```

Figure 6.14 Counts of Both, First, Second, and Neither.
See paragraph 7.2 for explanation.

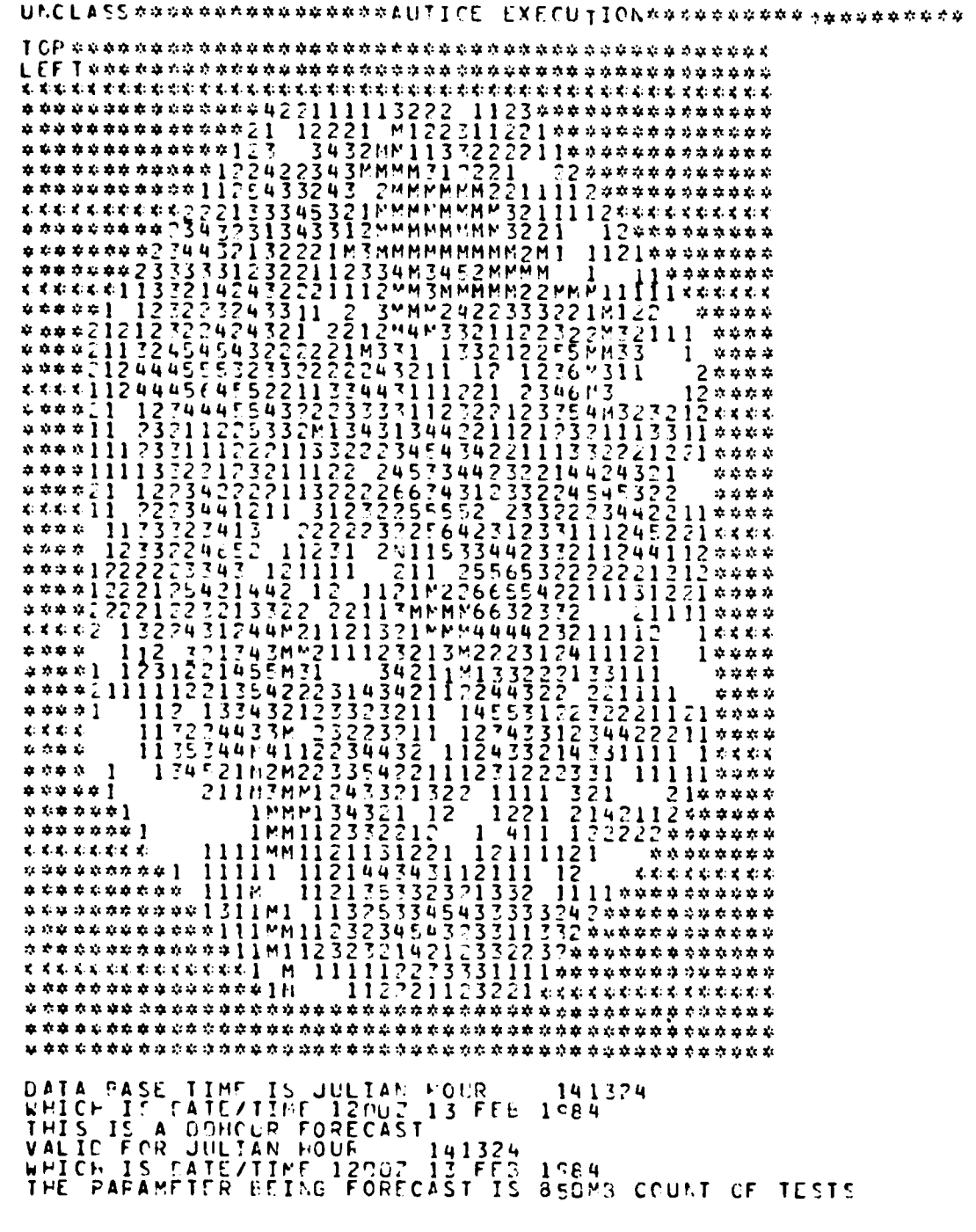

Figure 6.15 Counts of Tests Passed at Each Point. Numbers indicate how many of the six criteria are met at each point. Blank points had no criteria met.

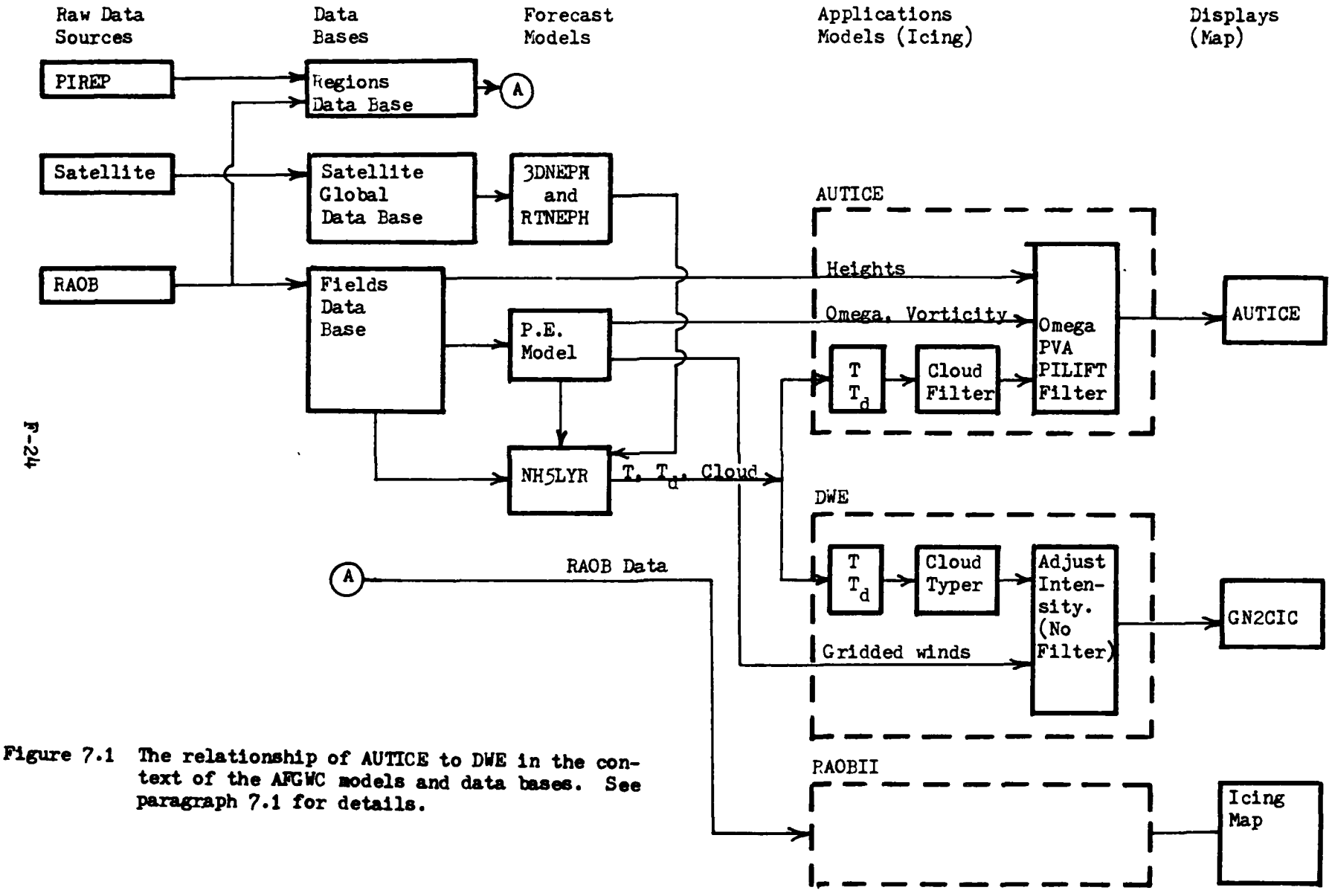

Figure 7.1 The relationship of AUTICE to DWE in the context of the AFGWC models and data bases. See paragraph 7.1 for details.

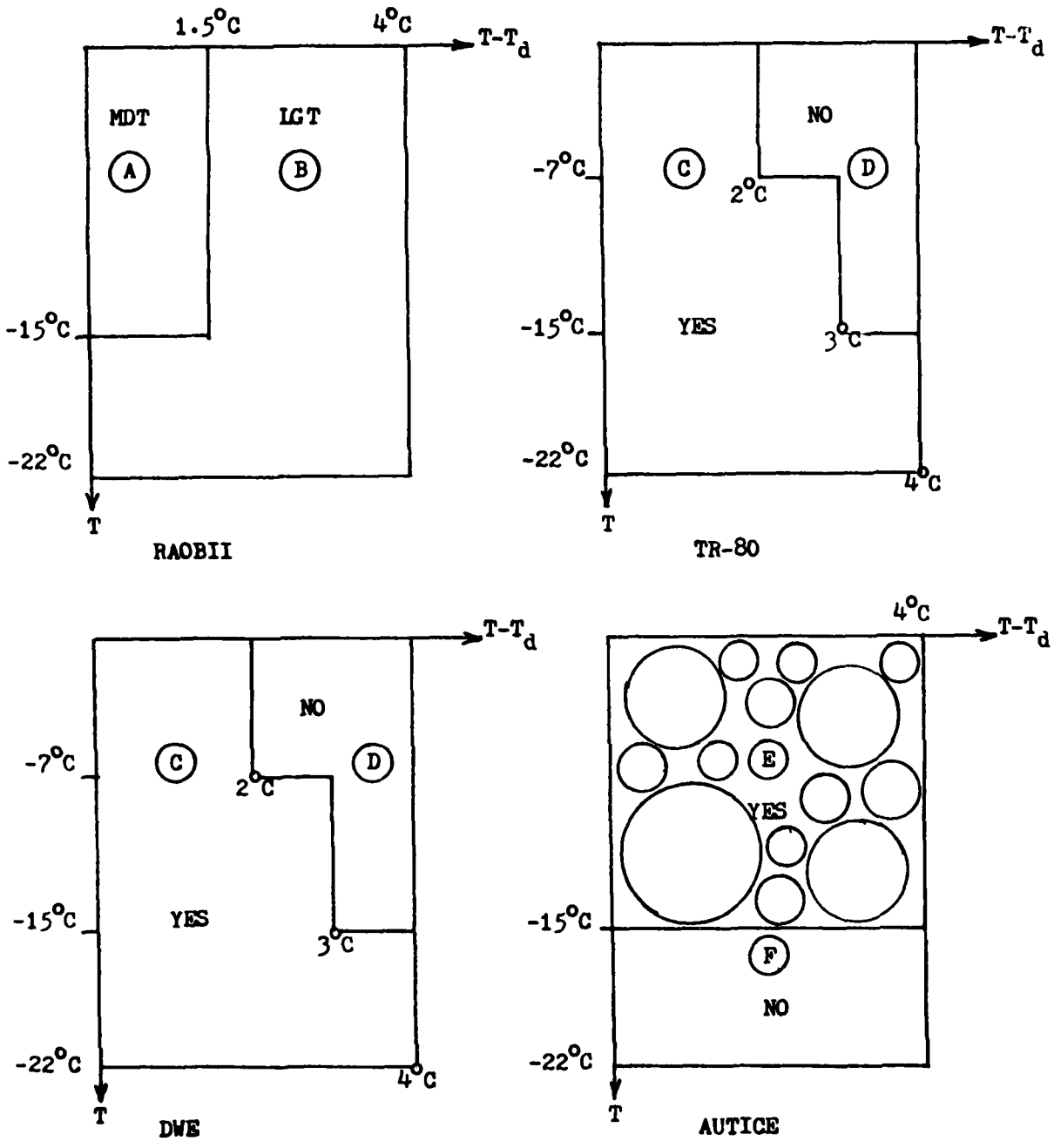

Figure 7.2 Temperature and dew-point icing forecast cut-offs in degrees Celsius for RAOBII, TR-80, DWE, and AUTICE. "MDT" and "LGT" imply moderate and light icing respectively.

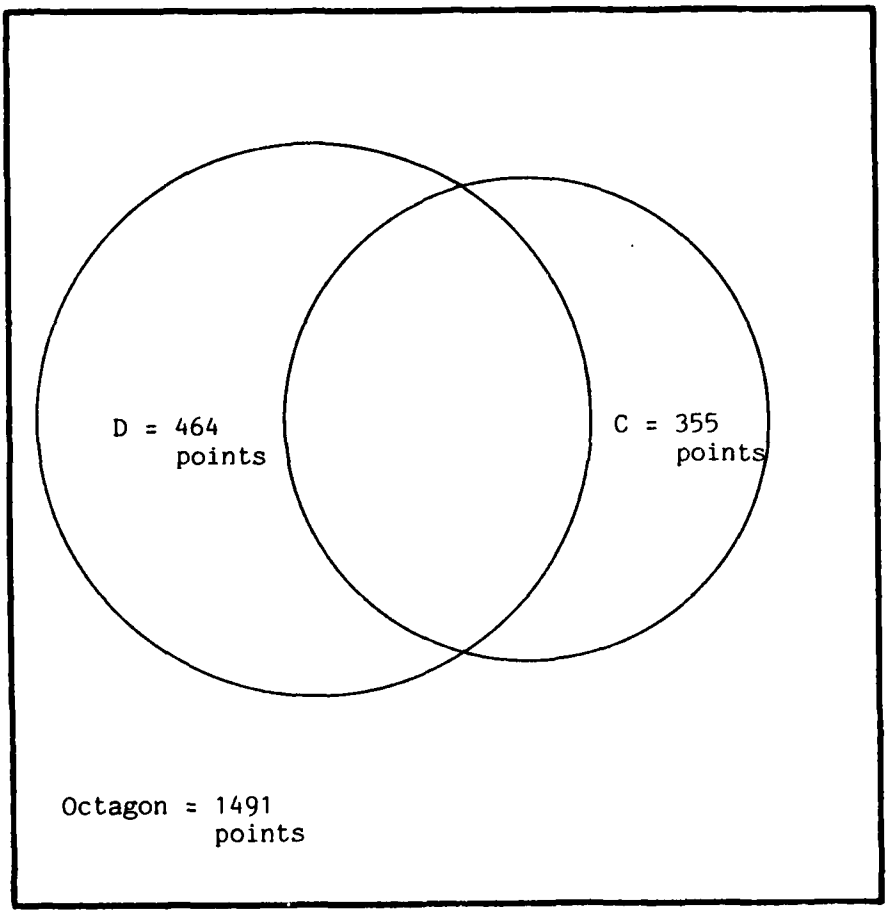

Figure 7.3 Proportional area representations of the numbers of points at 850mb meeting the dew-point criterion (464 points) and the cloud criterion (355 points). The boxed area is proportional to the 1491 AUTICE octagon points. The raw data for this figure was derived from Fig. 6.14.

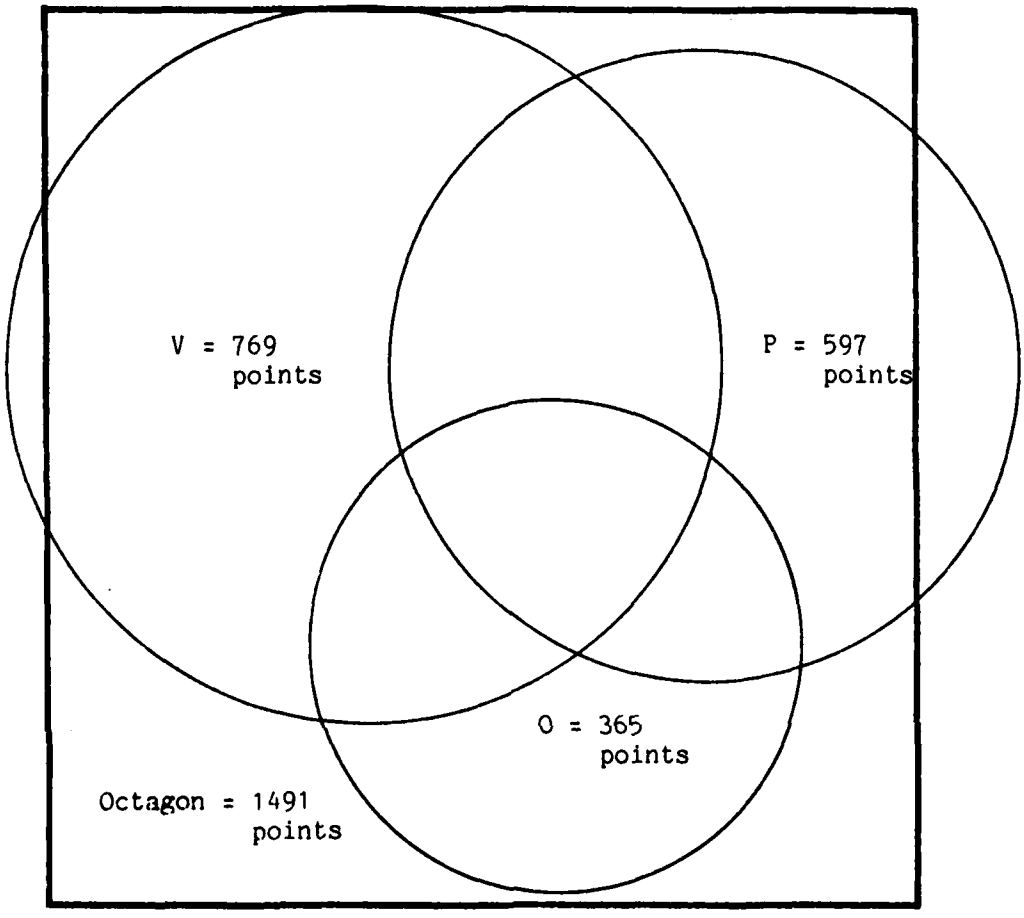

Figure 7.4 Proportional area representation of the numbers of points at 850mb meeting the vorticity advection criterion (769 points), the PILIFT criterion in either the lower or upper level (697 points), or the omega criterion (365 points). The boxed area is proportioned to represent the 1491 AUTICE octagon points. The raw data for this figure was derived from Fig. 6.14.

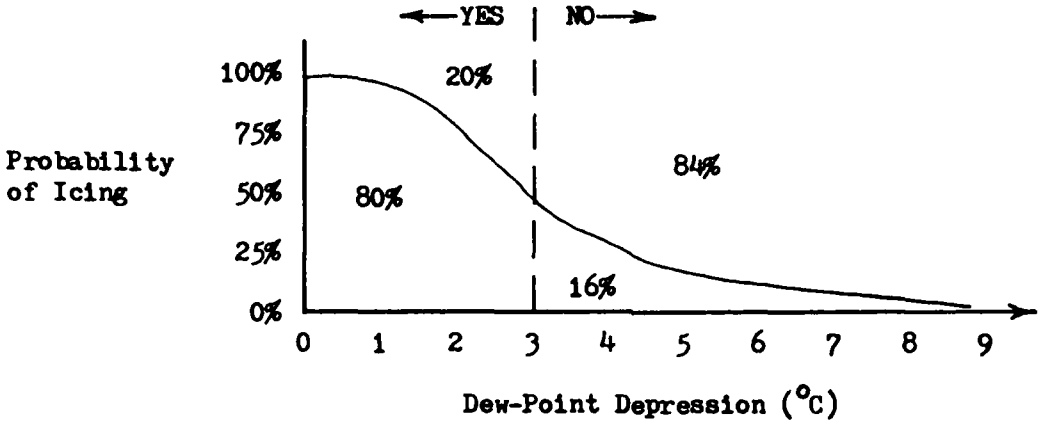

Figure 7.5 A graphical interpretation of the probability density curve for icing forecasts based on TR-80 paragraph 22.a and Table 2. Using a 3°C dew-point depression cut-off for forecasting icing, one would expect 20% of the YES forecasts to be false alarms and 80% to be hits. Similarly, 84% of the NO forecasts would be hits and 16% misses.

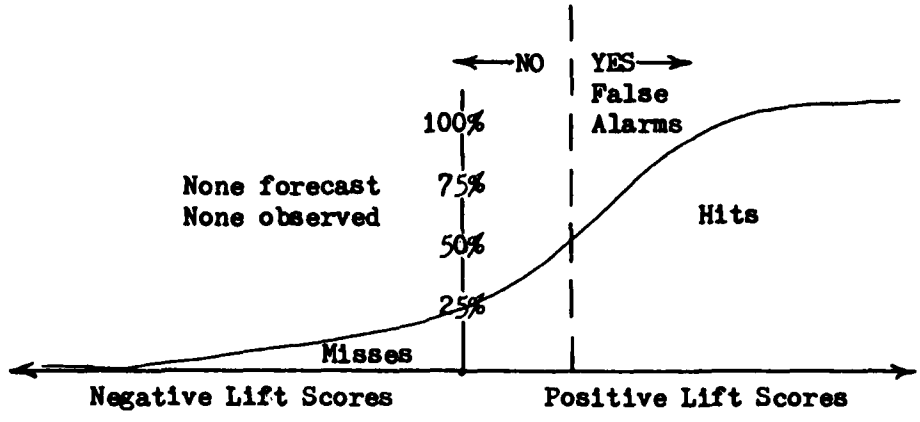

Figure 7.6 Hypothetical probability density curve which might be derived from future empirical studies relating AFGWC lift criteria to icing.

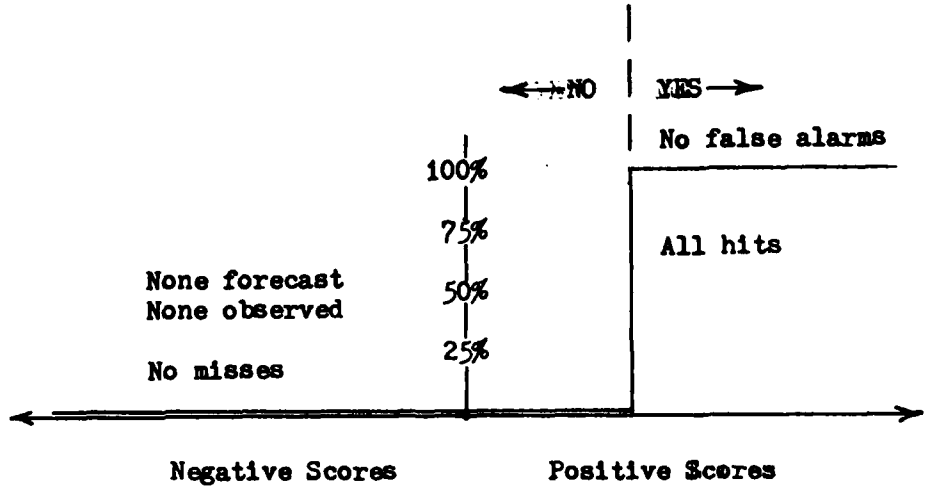

Figure 7.7 Hypothetical probability density curve required for perfect skill scores.

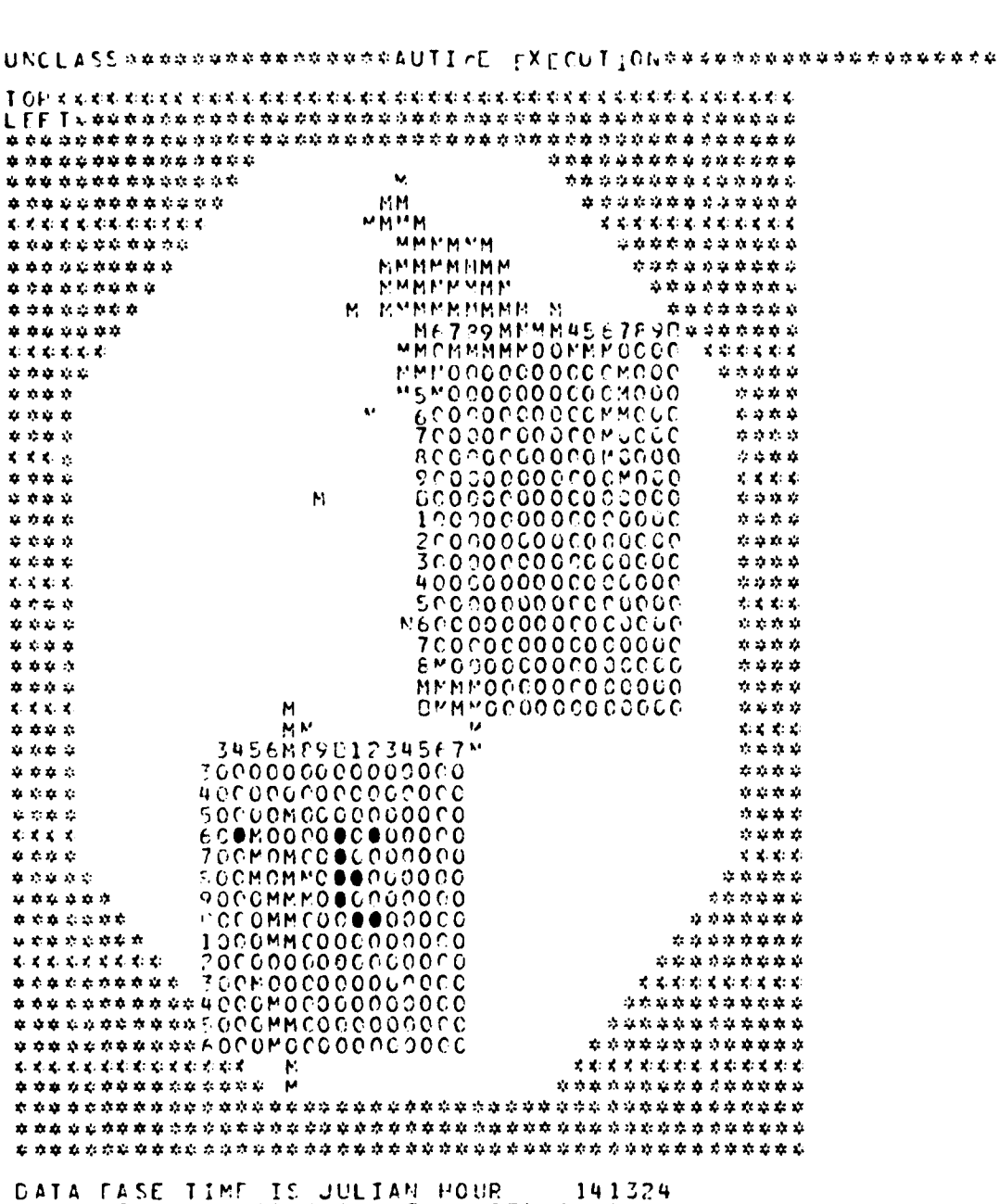

Figure 7.8 RAOBII Analyzed Icing over the CONUS BLM.

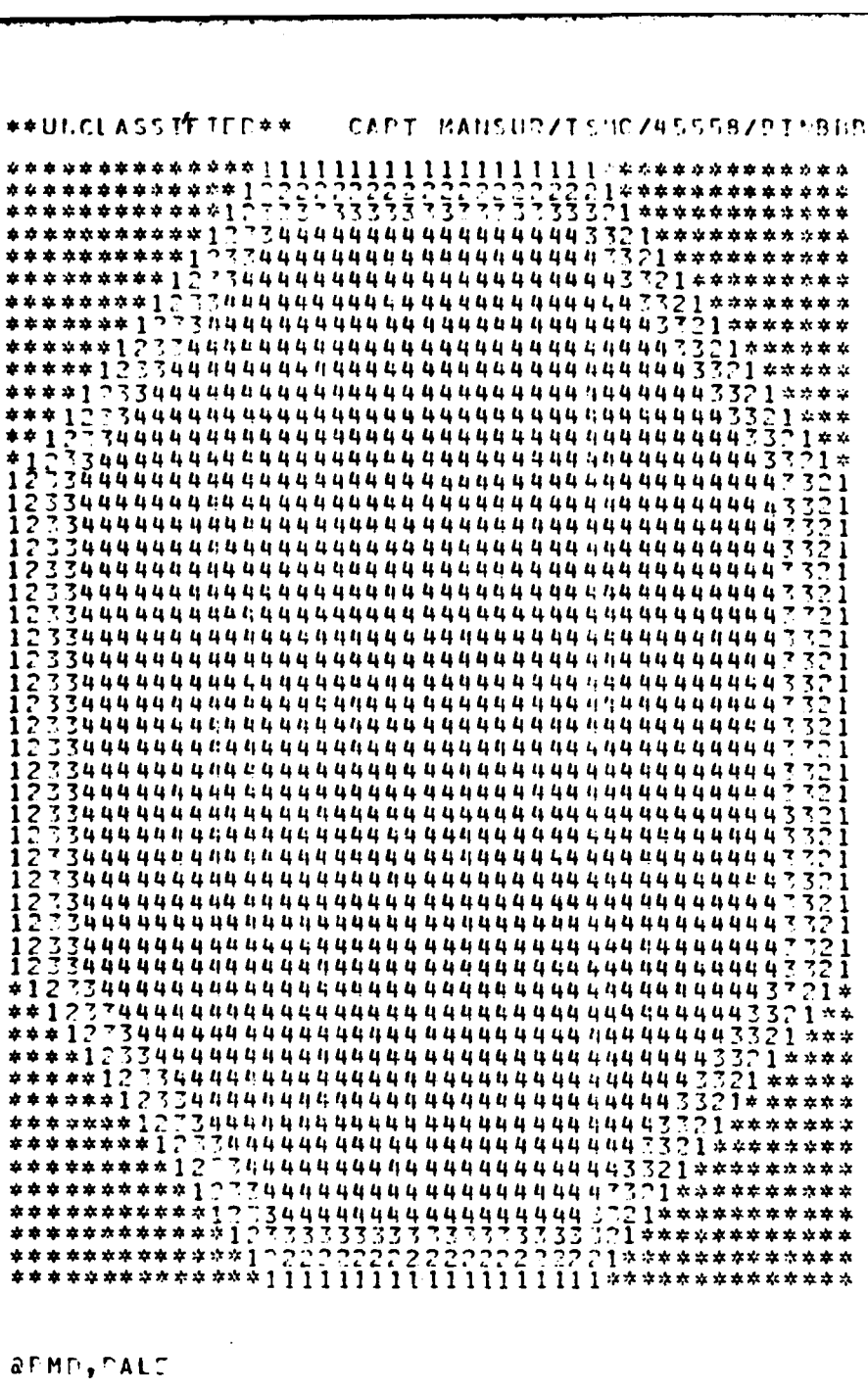

Figure A.1 The AFGWC whole mesh octagon (points inside the *'s) and the AUTICE octagon (points indicated by 4's).

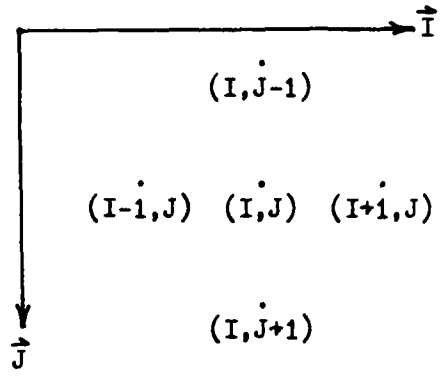

Figure C.1 Geometry for the computation of height gradients on a grid.

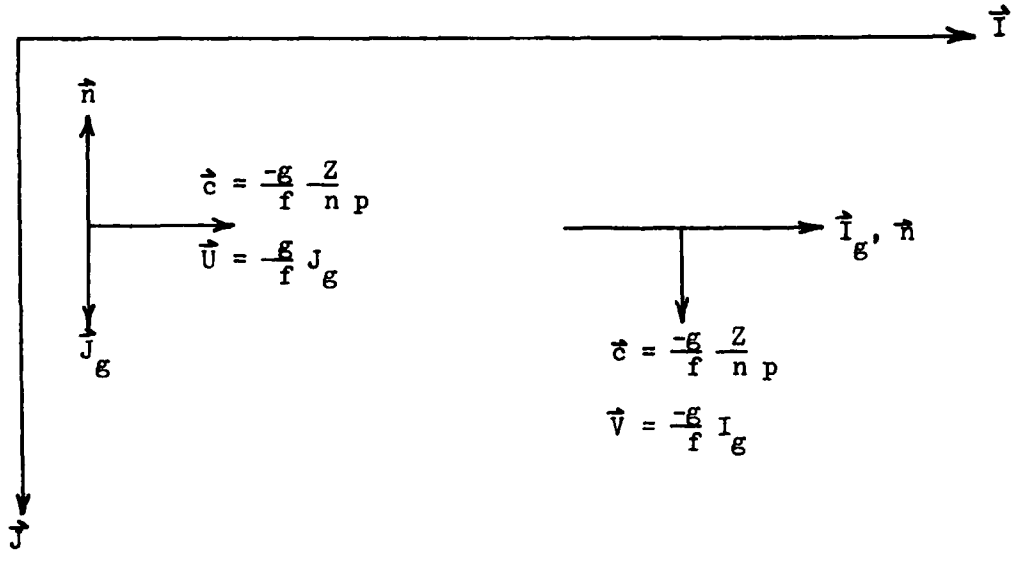

Figure C.2 Geometry for the computation of geostrophic wind components in the grid I and J directions using the natural coordinate system.

DISTRIBUTION:

1WW (1)
2WW (1)
3WW (1)
4WW (1)
5WW (1)
7WW (1)
AWS/DNT (1)
2WS (1)
AFGWC (5)
USAFETAC/DN (1)
USAFETAC/OL-A (1)
USAFETAC/TS (5)

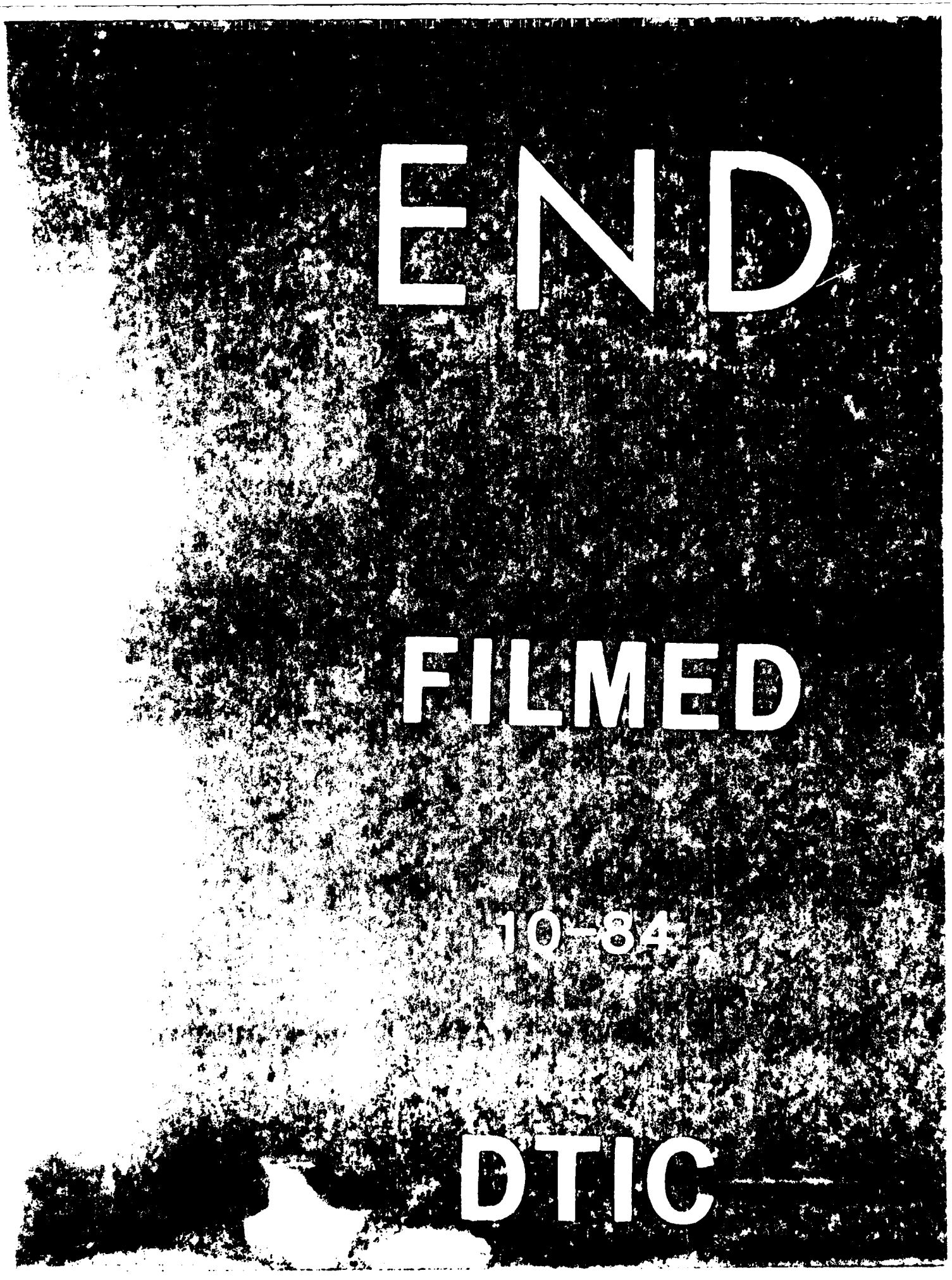
END
FILMED
10-84
DTIC